ELSEVIER

Applied Numerical Mathematics 13 (1993) 383–422

APPLIED NUMERICAL MATHEMATICS

Computational algorithms for aerodynamic analysis and design *

Antony Jameson **

Princeton University, School of Engineering and Applied Science, Department of Mechanical and Aerospace Engineering, P.O. Box CN5263, Princeton, NJ 08544-5263, USA

This paper is dedicated to Jacques Louis Lions, in honor of his extraordinary contributions not only to mathematics, but also in demonstrating the crucial role that mathematics of the highest order can play throughout pure and applied science.

1. Introduction

While the applications of computational fluid dynamics are pervasive throughout applied science and engineering, ranging from astrophysics to the design of cooling systems for semi-conductors, its role in aircraft design is crucial to an unusual extent, because of the narrow margins within which aircraft can operate efficiently. If computational aerodynamics is to be truly effective in the design process, it must be able to provide reliable answers rapidly and with low computational costs. With this in mind, the requirements can be identified as follows in a hierarchy of ascending difficulty:

(1) to calculate the flow with sufficient accuracy to permit design decisions to be made with confidence;
(2) to calculate the flow fast enough to allow interactive design and analysis;
(3) to embed the flow calculations in numerical optimization procedures which will automatically lead to improved designs.

This paper addresses some of the mathematical questions which underlie the realization of these goals, with a particular focus on two issues. The calculation of compressible flows at

* Contribution to the INRIA 25th Anniversary Conference on Computer Science and Control.
** Fax: (609) 258-1939.

SSDI 0168-9274(93)E0045-4

transonic, supersonic and hypersonic Mach numbers requires the implementation of non-oscillatory discrete schemes which combine high accuracy with high resolution of shock waves and contact discontinuities. These schemes must also be formulated in such a way that they allow the treatment of complex geometric shapes. This is needed for the realization of the first goal. Beyond this, the realization of the second goal requires schemes which converge rapidly to steady state solutions, and can also efficiently treat unsteady flows.

The first part of this paper presents a study of upwind biasing, artificial diffusion, and multigrid acceleration. The analysis leads to a construction of flux-limited dissipation for multi-dimensional structured and unstructured meshes which guarantees the positivity of a solution of a scalar conservation law, because a maximum cannot increase and a minimum cannot decrease. Numerical results are presented for several schemes which are both accurate and rapidly convergent. The aim of this work is to develop schemes which treat convection with a minimum amount of artificial diffusion. This is also a crucial building block for the treatment of viscous flows, because the attainment of acceptable accuracy is then contingent on the use of schemes with levels of artificial diffusion which are negligible in comparison with the true viscous terms.

The second part of the paper examines the question of automatic design. Here it is suggested that there are benefits to be gained by regarding the problem as the optimal control of a system governed by the partial differential equations of the flow, with boundary control implemented by movement of the boundary. This brings the problem within the framework of the theory of control of systems governed by partial differential equations, as it has been developed by J.L. Lions [22]. Some results of a feasibility study for transonic airfoil design are presented. Since the flow must be repeatedly recalculated, it is essential to minimize the computational cost, and a potential flow model was used for this study.

2. Algorithms for compressible flow with shock waves

2.1. Local extremum diminishing (LED) schemes with positive coefficients

Consider the discretization of a time-dependent conservation law such as

$$\frac{\partial v}{\partial t} + \frac{\partial}{\partial x} f(v) + \frac{\partial}{\partial y} g(v) = 0 \tag{1}$$

for a scalar dependent variable v on an arbitrary (possibly unstructured) mesh. Assuming that the mesh points are numbered in some way, let v_j be the value at mesh point j. Suppose that the approximation to (1) can be expressed in semi-discrete form in terms of differences between v_j and other mesh values v_k as

$$\frac{\mathrm{d}v_j}{\mathrm{d}t} = \sum_k c_{kj}(v_k - v_j).$$

If the scheme is supported by a compact stencil of points, c_{kj} will be zero for most values of k. Let the coefficients satisfy the positivity condition

$$c_{kj} \geqslant 0. \tag{2}$$

Then, if v_j is a local maximum (over the stencil of the difference scheme), $v_k - v_j \leqslant 0$, with the consequence that $\mathrm{d}v_j/\mathrm{d}t \leqslant 0$. Thus a local maximum cannot increase, and similarly a local minimum cannot decrease. Such a scheme will be called local extremum diminishing (LED).

This criterion was proposed by the author [13,14,18] as a convenient basis for the construction of non-oscillatory schemes on unstructured meshes. It assures positivity, because if v is everywhere positive, then its global minimum is positive, and this cannot decrease. When specialized to one dimension it also leads to the class of total variation diminishing (TVD) schemes proposed by Harten [8]. The total variation of v is

$$TV(v) = \int_{-\infty}^{\infty} \left| \frac{\mathrm{d}v}{\mathrm{d}x} \right| \mathrm{d}x,$$

that is, the sum of the absolute values of the variation over each upward and downward segment. It was observed by Laney and Caughey [20] that each extremum appears in the variation of the segment on each side of that extremum, with the consequence that

$$TV(v) = 2\Big(\sum \text{maxima} - \sum \text{minima}\Big),$$

if the end values are fixed. Thus, if a one-dimensional scheme is LED, it is also TVD. However, the TVD criterion does not readily generalize to multi-dimensional problems, whereas the LED criterion can be directly applied to multi-dimensional problems on both structured and unstructured meshes.

If the one-dimensional scalar conservation law

$$\frac{\partial v}{\partial t} + \frac{\partial}{\partial x} f(v) = 0 \tag{3}$$

is represented by a three-point scheme

$$\frac{\mathrm{d}v_j}{\mathrm{d}t} = c^+_{j+1/2}(v_{j+1} - v_j) + c^-_{j-1/2}(v_{j-1} - v_j),$$

the scheme is TVD if

$$c^+_{j+1/2} \geqslant 0, \qquad c^-_{j-1/2} \geqslant 0. \tag{4}$$

Suppose that (3) is approximated in conservation form by the semi-discrete scheme

$$\Delta x \frac{\mathrm{d}v_j}{\mathrm{d}t} + (h_{j+1/2} - h_{j-1/2}) = 0, \tag{5}$$

where $h_{j+1/2}$ is the numerical flux between cells j and $j+1$, and Δx is the mesh interval. In a diffusive scheme $h_{j+1/2}$ may be calculated as

$$h_{j+1/2} = \tfrac{1}{2}(f_{j+1} + f_j) - \alpha_{j+1/2}(v_{j+1} - v_j),$$

where the second term is a diffusive flux of first order. If the wave speed $a(v) = \partial f/\partial v$ is approximated as

$$a_{j+1/2} = \begin{cases} \dfrac{f_{j+1} - f_j}{v_{j+1} - v_j}, & v_{j+1} \neq v_j, \\ \left.\dfrac{\partial f}{\partial v}\right|_{v_j}, & v_{j+1} = v_j, \end{cases}$$

then

$$h_{j+1/2} - h_{j-1/2} = \left(\tfrac{1}{2}a_{j+1/2} - \alpha_{j+1/2}\right)\Delta v_{j+1/2} + \left(\tfrac{1}{2}a_{j-1/2} + \alpha_{j-1/2}\right)\Delta v_{j-1/2},$$

where

$$\Delta v_{j+1/2} = v_{j+1} - v_j.$$

Thus the TVD condition (4) is satisfied if

$$\alpha_{j+1/2} \geqslant \tfrac{1}{2}|a_{j+1/2}|.$$

If one takes

$$\alpha_{j+1/2} = \tfrac{1}{2}|a_{j+1/2}|,$$

the diffusive flux becomes

$$d_{j+1/2} = \tfrac{1}{2}|a_{j+1/2}|\Delta v_{j+1/2}$$

and one obtains the first-order upwind scheme

$$h_{j+1/2} = \begin{cases} f_j, & \text{if } a_{j+1/2} > 0, \\ f_{j+1}, & \text{if } a_{j+1/2} < 0. \end{cases}$$

This is the least-diffusive first-order scheme which satisfies the TVD condition. In this sense upwinding is a natural approach to the construction of non-oscillatory schemes.

2.2. *Flux splitting*

Steger and Warming [27] first showed how to generalize the concept of upwinding to the system of conservation laws,

$$\frac{\partial w}{\partial t} + \frac{\partial}{\partial x} f(w) = 0, \tag{6}$$

by the concept of flux splitting. Suppose that the flux is split as $f = f^+ + f^-$ where $\partial f^+/\partial w$ and $\partial f^-/\partial w$ have positive and negative eigenvalues. Then the first-order upwind scheme is produced by taking the numerical flux to be

$$h_{j+1/2} = f_j^+ + f_{j+1}^-.$$

This can be expressed in viscosity form as

$$h_{j+1/2} = \tfrac{1}{2}(f^+_{j+1} + f^+_j) - \tfrac{1}{2}(f^+_{j+1} - f^+_j) + \tfrac{1}{2}(f^-_{j+1} + f^-_j) + \tfrac{1}{2}(f^-_{j+1} + f^-_j)$$
$$= \tfrac{1}{2}(f_{j+1} + f_j) - d_{j+1/2},$$

where the diffusive flux is

$$d_{j+1/2} = \tfrac{1}{2}\Delta(f^+ - f^-)_{j+1/2}. \tag{7}$$

Roe derived the alternative formulation of flux difference splitting [26] by distributing the corrections due to the flux difference in each interval upwind and downwind to obtain

$$\Delta x \frac{\mathrm{d}w_j}{\mathrm{d}t} + (f_{j+1} - f_j)^- + (f_j - f_{j-1})^+ = 0,$$

where now the flux difference $f_{j+1} - f_j$ is split. The corresponding diffusive flux is

$$d_{j+1/2} = \tfrac{1}{2}(\Delta f^+_{j+1/2} - \Delta f^-_{j+1/2}).$$

Following Roe's derivation, let $A_{j+1/2}$ be a mean value Jacobian matrix exactly satisfying the condition

$$f_{j+1} - f_j = A_{j+1/2}(w_{j+1} - w_j).$$

Then a splitting according to characteristic fields is obtained by decomposing $A_{j+1/2}$ as

$$A_{j+1/2} = T\Lambda T^{-1},$$

where the columns of T are the eigenvectors of $A_{j+1/2}$, and Λ is a diagonal matrix of the eigenvalues. Then

$$\Delta f^{\pm}_{j+1/2} = T\Lambda^{\pm}T^{-1}\Delta w_{j+1/2}.$$

Now the corresponding diffusive flux is

$$\tfrac{1}{2}|A_{j+1/2}|(w_{j+1} - w_j),$$

where

$$|A_{j+1/2}| = T|\Lambda|T^{-1}$$

and $|\Lambda|$ is the diagonal matrix containing the absolute values of the eigenvalues.

Simple stable schemes can be produced by the splitting

$$(f_{j+1} - f_j)^{\pm} = \tfrac{1}{2}(f_{j+1} - f_j) \pm \alpha_{j+1/2}(w_{j+1} - w_j),$$

which satisfies the positivity condition on the eigenvalues if $\alpha_{j+1/2} > \tfrac{1}{2}\max|\lambda(A_{j+1/2})|$ and corresponds to the scalar diffusive flux

$$d_{j+1/2} = \alpha_{j+1/2}\Delta w_{j+1/2}.$$

Characteristic splitting has the advantage that it allows a discrete shock structure with a single interior point.

2.3. High resolution switched scheme

Higher-order non-oscillatory schemes are generally derived by introducing anti-diffusive terms in a controlled manner. Anti-diffusive terms can be introduced by subtracting neighboring differences to produce a third-order diffusive flux

$$d_{j+1/2} = \alpha_{j+1/2}\left\{\Delta w_{j+1/2} - \tfrac{1}{2}\left(\Delta w_{j+3/2} + \Delta w_{j-1/2}\right)\right\}. \tag{8}$$

The positivity condition (2) is violated by this scheme. It generates substantial oscillations in the vicinity of shock waves which can be eliminated by switching locally to the first-order scheme. The switch introduced by Jameson, Schmidt and Turkel [19], which has proved effective for this purpose, has recently been improved by Swanson and Turkel [28]. Typically it is computed from the pressure, and the improved switch is taken as the maximum in some neighborhood of

$$Q_j = \left| \frac{\Delta p_{j+1/2} - \Delta p_{j-1/2}}{P_o + (1-\varepsilon)P_1 + \varepsilon P_2} \right|,$$

where

$$P_1 = |\Delta p_{j+1/2}| + |\Delta p_{j-1/2}|,$$

$$P_2 = |p_{j+1}| + 2|p_j| + |p_{j-1}|.$$

The value of ε is typically $\frac{1}{2}$, and P_o is a threshold to make sure that the denominator cannot be zero. Other quantities such as the entropy may be used to calculate the switch. The diffusive flux is now calculated as

$$d_{j+1/2} = \varepsilon^{(2)}_{j+1/2}\Delta w_{j+1/2} - \varepsilon^{(4)}_{j+1/2}\left(\Delta w_{j+3/2} - 2\Delta w_{j+1/2} + \Delta w_{j-1/2}\right),$$

where, if S is the maximum of Q in a neighborhood and $R_{j+1/2}$ is the spectral radius of $A_{j+1/2}$, then

$$\varepsilon^{(2)}_{j+1/2} = \min(\alpha_1, \alpha_2 S) R_{j+1/2},$$

$$\varepsilon^{(4)}_{j+1/2} = \max\left(0, \beta_1 - \beta_2 \varepsilon^{(2)}_{j+1/2}\right) R_{j+1/2}.$$

Usually $\alpha_1 = \frac{1}{2}$ and $\beta_1 = \frac{1}{4}$ to scale the diffusion to the level corresponding to upwinding, while α_2 and β_2 must be chosen to switch from third-order to first-order diffusion fast enough near a shock wave.

With this construction the role of the high-order diffusion is to provide global damping of oscillatory modes which would otherwise inhibit convergence to a steady state, while the role of the first-order diffusion is to control oscillations near discontinuities. Numerical experiments with multigrid acceleration confirm that the rate of convergence to a steady state is essentially the same when the first-order diffusion is eliminated, but large pre- and post-shock oscillations appear in the solution. On the other hand the multigrid scheme will not converge if the global diffusion is eliminated. Fast convergence and highly resolved shock waves can be obtained by using characteristic splitting in a first-order scheme, but the accuracy is unacceptably low, even on meshes as fine as 320×64 cells. The switched scheme has proved successful in the calculation of steady compressible flows over a wide range of Mach numbers, provided that it is

combined with an appropriate construction of the basic first-order diffusive terms. A formulation which proves to be particularly effective at high Mach numbers is presented in Section 2.6.

2.4. Symmetric limited positive (SLIP) scheme

An alternative route to high resolution without oscillation is to introduce flux limiters to guarantee the satisfaction of the positivity condition (2). The use of limiters dates back to the work of Boris and Book [2]. A particularly simple way to introduce limiters, proposed by the author in 1984 [12], is to use flux-limited dissipation. In this scheme the third-order diffusion defined by equation (8) is modified by the insertion of limiters which produce an equivalent three-point scheme with positive coefficients. The original scheme can be improved in the following manner so that less restrictive flux limiters are required. Let $L(u, v)$ be a limited average of u and v with the following properties:

(P1) $L(u, v) = L(v, u)$;
(P2) $L(\alpha u, \alpha v) = \alpha L(u, v)$;
(P3) $L(u, u) = u$;
(P4) $L(u, v) = 0$, if u and v have opposite signs.

Properties (P1)–(P3) are natural properties of an average. Property (P4) is needed for the construction of an LED or TVD scheme.

It is convenient to introduce the notation

$$\phi(r) = L(1, r) = L(r, 1).$$

Then it follows from (P2) that

$$L(u, v) = \phi\left(\frac{v}{u}\right)u = \phi\left(\frac{u}{v}\right)v.$$

Also it follows on setting $v = 1$ and $u = r$ that

$$\phi(r) = r\phi\left(\frac{1}{r}\right).$$

Thus, if there exists $r < 0$ for which $\phi(r) > 0$, then $\phi(1/r) < 0$. The only way to ensure that $\phi(r) \geqslant 0$ is to require $\phi(r) = 0$ for all $r < 0$, corresponding to property (P4).

Now one defines the diffusive flux for a scalar conservation law as

$$d_{j+1/2} = \alpha_{j+1/2}\left\{\Delta v_{j+1/2} - L\left(\Delta v_{j+3/2}, \Delta v_{j-1/2}\right)\right\}. \tag{9}$$

Also define

$$r^+ = \frac{\Delta v_{j+3/2}}{\Delta v_{j-1/2}}, \qquad r^- = \frac{\Delta v_{j-3/2}}{\Delta v_{j+1/2}}.$$

Then, the scalar scheme (5) reduces to

$$\begin{aligned}\Delta x\frac{dv_j}{dt} &= -\tfrac{1}{2}a_{j+1/2}\Delta v_{j+1/2} - \tfrac{1}{2}a_{j-1/2}\Delta v_{j-1/2}\\ &\quad + \alpha_{j+1/2}\left(\Delta v_{j+1/2} - \phi(r^+)\Delta v_{j-1/2}\right) - \alpha_{j-1/2}\left(\Delta v_{j-1/2} - \phi(r^-)\Delta v_{j+1/2}\right)\\ &= \left\{\alpha_{j+1/2} - \tfrac{1}{2}a_{j+1/2} + \alpha_{j-1/2}\phi(r^-)\right\}\Delta v_{j+1/2}\\ &\quad - \left\{\alpha_{j-1/2} + \tfrac{1}{2}a_{j-1/2} + \alpha_{j+1/2}\phi(r^+)\right\}\Delta v_{j-1/2}.\end{aligned}$$

Thus the scheme satisfies the TVD condition if $\alpha_{j+1/2} \geqslant \frac{1}{2}|a_{j+1/2}|$ for all j, and $\phi(r) \geqslant 0$, which is assured by property (P4) on L. At the same time it follows from property (P3) that the first-order diffusive flux is cancelled when Δv is smoothly varying and of constant sign.

The new scheme will be referred to as the symmetric limited positive (SLIP) scheme. The construction benefits from the fact that the terms involving $\phi(r^-)$ and $\phi(r^+)$ reinforce the positivity of the coefficients whenever ϕ is positive. Thus the only major restriction on $L(u, v)$ is that it must be zero when u and v have opposite signs, or that $\phi(r) = 0$ when $r < 0$. If $\Delta v_{j+3/2}$ and $\Delta v_{j-1/2}$ have opposite signs, then there is an extremum at either j or $j+1$. In the case of an odd–even mode, however, they have the same sign, which is opposite to that of $\Delta v_{j+1/2}$, so that they reinforce the damping in the same way that a simple central fourth-difference formula would. At the crest of a shock, if the upstream flow is constant then $\Delta v_{j-1/2} = 0$, and thus $\Delta v_{j+3/2}$ is prevented from cancelling any part of $\Delta v_{j+1/2}$ because it is limited by $\Delta v_{j-1/2}$.

A variety of limiters may be defined which meet the requirements of properties (P1)–(P4). Define

$$S(u, v) = \tfrac{1}{2}\{\text{sign}(u) + \text{sign}(v)\},$$

so that

$$S(u, v) = \begin{cases} 1, & \text{if } u > 0 \text{ and } v > 0,\\ 0, & \text{if } u \text{ and } v \text{ have opposite sign},\\ -1, & \text{if } u < 0 \text{ and } v < 0.\end{cases}$$

Three limiters which are appropriate are the following well-known schemes:

(1) *minmod*:

$$L(u, v) = S(u, v)\,\min(|u|, |v|);$$

(2) *Van Leer*:

$$L(u, v) = S(u, v)\frac{2|u||v|}{|u| + |v|};$$

(3) *superbee*:

$$L(u, v) = S(u, v)\,\max\{\min(2|u|, |v|), \min(|u|, 2|v|)\}.$$

These are special cases of the following more general formulas:

(4) *α-mod*:

$$L(u, v) = S(u, v)\frac{(1+\alpha)|u||v|}{\max(|u|,|v|) + \alpha \min(|u|,|v|)};$$

(5) *α-β-mod*:

$$L(u, v) = S(u, v)\frac{(1+\alpha)|u|^{(\beta+1)/2}|v|^{(\beta+1)/2}}{\max(|u|^{\beta},|v|^{\beta}) + \alpha \min(|u|^{\beta},|v|^{\beta})};$$

(6) *α-bee*:

$$L(u, v) = S(u, v) \max\{\min(\alpha|u|,|v|), \min(|u|, \alpha|v|)\}.$$

α-mod reduces to minmod when $\alpha = 0$, and to Van Leer when $\alpha = 1$. α-β-mod reduces to the geometric mean when $\beta = 0$ and u and v have the same sign, and to α-mod when $\beta = 1$. α-bee reduces to minmod when $\alpha = 1$ and to superbee when $\alpha = 2$. Another formulation is simply to limit the arithmetic mean by some multiple of the smaller of $|u|$ and $|v|$:

(7) *α-mean*:

$$L(u, v) = S(u, v) \min(\tfrac{1}{2}|u+v|, \alpha|u|, \alpha|v|).$$

2.5. SLIP schemes on multi-dimensional unstructured meshes

Consider the discretization of the scalar conservation law (1) by a scheme in which v is represented at the vertices of a triangular mesh, as sketched in Fig. 1. In a finite volume approximation (1) is written in integral form as

$$\frac{\partial}{\partial t}\int v \, ds + \oint f(v)\, dx - g(v)\, dy,$$

and this is approximated by trapezoidal integration around a polygon consisting of the triangles with a common vertex, o, say.

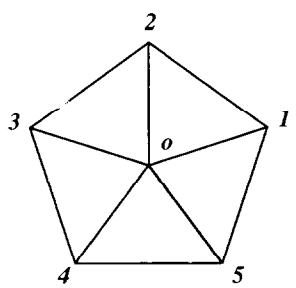

Fig. 1. Cell surrounding vertex o.

Thus (1) is discretized as

$$S\frac{dv_o}{dt} + \tfrac{1}{2}\sum_k \{(f_k + f_{k-1})(y_k - y_{k-1}) - (g_k + g_{k-1})(x_k - x_{k-1})\} = 0$$

where $f_k = f(v_k)$, $g_k = g(v_k)$, S is the area of the polygon, and k ranges over its vertices. This may be rearranged as

$$S\frac{dv_o}{dt} + \sum_k (f_k \Delta y_k - g_k \Delta x_k) = 0,$$

where

$$\Delta x_k = \tfrac{1}{2}(x_{k+1} - x_{k-1}), \qquad \Delta y_k = \tfrac{1}{2}(y_{k+1} - y_{k-1}).$$

Following, for example, [13,18], this may now be reduced to a sum of differences over the edges ko by noting that $\sum_k \Delta x_k = \sum_k \Delta y_k = 0$. Consequently f_o and g_o may be added to give

$$S\frac{dv_o}{dt} + \sum \{(f_k - f_o)\Delta y_k - (g_k - g_o)\Delta x_k\} = 0. \tag{10}$$

Define the coefficient a_{ko} as

$$a_{ko} = \begin{cases} \dfrac{(f_k - f_o)\Delta y_k - (g_k - g_o)\Delta x_k}{\Delta v_{ko}}, & v_k \neq v_o, \\ \left(\dfrac{\partial f}{\partial v}\Delta y_k - \dfrac{\partial g}{\partial v}\Delta x_k\right)\Big|_{v = v_o}, & v_k = v_o, \end{cases}$$

and

$$\Delta v_{ko} = v_k - v_o.$$

Then equation (10) reduces to

$$S\frac{dv_o}{dt} + \sum_k a_{ko}\Delta v_{ko} = 0.$$

To produce a scheme satisfying the sign condition (2), add a dissipative term on the right-hand side of the form

$$\sum_k \alpha_{ko}\Delta v_{ko}, \tag{11}$$

where the coefficients α_{ko} satisfy the condition

$$\alpha_{ko} \geqslant |a_{ko}|. \tag{12}$$

The extension to a system of conservation laws, as defined by equation (6), can be carried out with the aid of Roe's construction [26]. Now a_{ko} is replaced by the corresponding matrix A_{ko} such that

$$A_{ko}(w_k - w_o) = (f_k - f_o)\Delta y_k - (g_k - g_o)\Delta x_k.$$

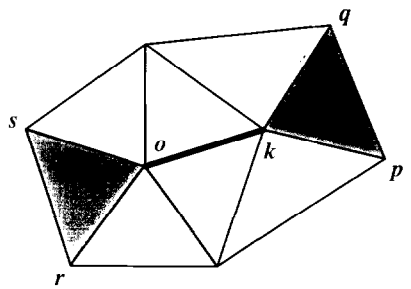

Fig. 2. Edge ko and adjacent triangles.

Suppose that A_{ko} is decomposed as $T\Lambda T^{-1}$ where the columns t_j of T are the eigenvectors of A_{ko}. Then the difference $\Delta w = w_k - w_o$ is expressed as a sum $\Sigma_j \alpha_j t_j$ of the eigenvectors, where the coefficients $\alpha_j = (T^{-1}\Delta w)_j$ represent the characteristic variables, and the diffusive term along the edge ko is constructed as

$$|A_{ko}|\Delta w = T|\Lambda|T^{-1}\Delta w.$$

These simple schemes are far too dissipative. Anti-diffusive terms may be added without violating the positivity condition (2) by the following generalization of the one-dimensional scheme. Considering again the scalar case, let $\boldsymbol{l}_{ko}$ be the vector connecting the edge ko and define the neighboring differences

$$\Delta^+ v_{ko} = \boldsymbol{l}_{ko} \cdot \nabla^+ v, \qquad \Delta^- v_{ko} = \boldsymbol{l}_{ko} \cdot \nabla^- v,$$

where $\nabla^{\pm} v$ are the gradients of v evaluated in the triangles out of which and into which $\boldsymbol{l}_{ko}$ points, as sketched in Fig. 2. Arminjon and Dervieux have used a similar definition [1].

It may now be verified that

$$\Delta^+ v_{ko} = \varepsilon_{pk}(v_p - v_k) + \varepsilon_{qk}(v_q - v_k)$$

and

$$\Delta^- v_{ko} = \varepsilon_{or}(v_o - v_r) + \varepsilon_{os}(v_o - v_s),$$

where the coefficients ε_{pk}, ε_{qk}, ε_{or}, and ε_{os} are all non-negative. Now define the diffusive term for the edge ko as

$$d_{ko} = \alpha_{ko}\{\Delta v_{ko} - L(\Delta^+ v_{ko}, \Delta^- v_{ko})\}, \tag{13}$$

where $L(u, v)$ is a limited average with the properties (P1)–(P4) that were defined in Section 2.4. In considering the sum of the terms at the vertex o write

$$L(\Delta^+ v_{ko}, \Delta^- v_{ko}) + \phi(r^+_{ko})\Delta^- v_{ko},$$

where

$$r^+_{ko} = \frac{\Delta^+ v_{ko}}{\Delta^- v_{ko}}.$$

Then, since the coefficients ε_{or} and ε_{os} are non-negative, and $\phi(r_{ko}^{+})$ is non-negative, the limited anti-diffusive term in (13) produces a contribution from every edge which reinforces the positivity condition (2). Similarly, in considering the sum of the terms at k one writes

$$L(\Delta^{+}v_{ko}, \Delta^{-}v_{ko}) = \phi(r_{ko}^{-})\Delta^{+}v_{ko},$$

where

$$r_{ko}^{-} = \frac{\Delta^{-}v_{ko}}{\Delta^{+}v_{ko}},$$

and again the discrete equation receives a contribution with the right sign. One may therefore deduce the following result:

Theorem 1 (Positivity Theorem). *Suppose that the discrete conservation law* (10) *is augmented by flux-limited dissipation following equations* (11) *and* (13). *Then the positivity condition* (12), *together with the properties* (P1)–(P4) *for limited averages, are sufficient to ensure that a maximum cannot increase and a minimum cannot decrease at any interior mesh point.*

Note also that, if this construction is applied to any linear function v, then

$$\Delta v_{ko} = \Delta^{+}v_{ko} = \Delta^{-}v_{ko},$$

with the consequence that the contribution of the diffusive terms is exactly zero. In the case of a smoothly varying function v, suppose that $\boldsymbol{l}_{ko} \cdot \nabla v \neq 0$ and the limiter is smooth in the neighborhood of $r_{ko}^{\pm} = 1$. Then substitution of a Taylor series expansion indicates that the magnitude of the diffusive flux will be of second order. At an extremum the anti-diffusive term is cut off and the diffusive flux is of first order.

The three-dimensional conservation law

$$\frac{\partial v}{\partial t} + \frac{\partial}{\partial x} f(v) + \frac{\partial}{\partial y} g(v) + \frac{\partial}{\partial z} h(v) = 0 \tag{14}$$

can be treated in a similar manner by first expressing the convective flux balance as a sum of differences along edges. Consider the set of tetrahedrons containing a common edge. Then one may associate with that edge a vector area $\boldsymbol{S}$ which is one-third the sum of the areas of the set of faces which form one of two opposing umbrellas around the edge. With a notation similar to that of Fig. 1 the convective flux balance corresponding to equation (14) at an interior mesh point may be written as

$$V\frac{\mathrm{d}v_o}{\mathrm{d}t} + \sum_k (\boldsymbol{F}_k - \boldsymbol{F}_o) \cdot \boldsymbol{S}_{ko} = 0, \tag{15}$$

where the columns of $\boldsymbol{F}$ are the flux vectors f, g and h, and V is the volume of the polyhedron formed by the union of all the tetrahedrons with the common vertex o. Here $\boldsymbol{F}_o$ may be added or subtracted since $\sum_k \boldsymbol{S}_{ko} = \boldsymbol{0}$. Diffusion may now be added along the edges in exactly the same way as before. When the convective flux balance is evaluated, it is more convenient to use the

sum $\Sigma_k(\boldsymbol{F}_k + \boldsymbol{F}_o) \cdot \boldsymbol{S}_{ko}$, so that the convective flux along each edge needs to be calculated only once in a loop over the edges and appropriately accumulated at nodes k and o.

At boundary points equations (10) or (15) need to be augmented by additional fluxes through the boundary edges or faces. The first-order diffusive flux $\alpha_{ko}\Delta v_{ko}$ may be offset by subtracting an anti-diffusive flux evaluated from the interior, taking a limited average with Δv_{ko}.

2.6. *Construction of convective upwind and split pressure (CUSP) schemes*

Discrete schemes should be designed to provide high accuracy in smooth regions in combination with oscillation-free shocks at the lowest possible computational cost. This in turn requires both economy in the formulation, and in the case of steady state calculations, a rapidly convergent iterative scheme. The convective upwind and split pressure (CUSP) scheme described below meets these requirements, while providing excellent shock resolution at high Mach numbers. When very sharp resolution of weak shocks is required, the results can be improved by characteristic splitting with matrix diffusion using Roe averaging.

Consider the one-dimensional equations for gas dynamics. In this case the solution and flux vectors appearing in equation (6) are

$$w = \begin{pmatrix} \rho \\ \rho u \\ \rho E \end{pmatrix}, \qquad f = \begin{pmatrix} \rho u \\ \rho u^2 + p \\ \rho u H \end{pmatrix},$$

where ρ is the density, u is the velocity, E is the total energy, p is the pressure, and H is the stagnation enthalpy. If γ is the ratio of specific heats and c is the speed of sound

$$p = (\gamma - 1)\rho\left(E - \frac{u^2}{2}\right), \qquad c^2 = \frac{\gamma p}{\rho}, \qquad H = E + \frac{p}{\rho} = \frac{c^2}{\gamma - 1} + \frac{u^2}{2}.$$

In a steady flow H is constant. This remains true for the discrete scheme only if the diffusion is constructed so that it is compatible with this condition.

The eigenvalues of the Jacobian matrix $A = \partial f / \partial w$ are u, $u + c$, and $u - c$. If $u > 0$ and the flow is locally supersonic ($M = u/c > 1$), then all the eigenvalues are positive, and simple upwinding is thus a natural choice for diffusion in supersonic flow. It is convenient to consider the convective and pressure fluxes

$$f_c = u\begin{pmatrix} \rho \\ \rho u \\ \rho H \end{pmatrix} = u w_c, \qquad f_p = \begin{pmatrix} 0 \\ p \\ 0 \end{pmatrix}$$

separately. Upwinding of the convective flux is achieved by

$$d_{p_{j+1/2}} = |u_{j+1/2}|\Delta w_{c_{j+1/2}} = |M|c_{j+1/2}\Delta w_{c_{j+1/2}},$$

where M is the local Mach number attributed to the interval. Upwinding of the pressure is achieved by

$$d_{j+1/2} = \operatorname{sign}(M)\begin{pmatrix} 0 \\ \Delta p_{j+1/2} \\ 0 \end{pmatrix}.$$

Full upwinding of both f_c and f_p is incompatible with stability in subsonic flow, since pressure waves with the speed $u-c$ would be traveling backwards, and the discrete scheme would not have a proper zone of dependence. Since the eigenvalues of $\partial f_c/\partial w$ are u, u and γu, while those of $\partial f_p/\partial w$ are 0, 0 and $-(\gamma-1)u$, a split with

$$f^+ = f_c, \qquad f^- = f_p$$

leads to a stable scheme, used by Denton [6], in which downwind differencing is used for the pressure.

This scheme does not reflect the true zone of dependence in supersonic flow. Thus one may seek a scheme with

$$d_{c_{j+1/2}} = f_1(M) c_{j+1/2} \Delta w_{c_{j+1/2}}, \qquad d_{p_{j+1/2}} = f_2(M) \begin{pmatrix} 0 \\ \Delta p_{j+1/2} \\ 0 \end{pmatrix},$$

where $f_1(M)$ and $f_2(M)$ are blending functions with the asymptotic behavior $f_1(M) \to |M|$ and $f_2(M) \to \text{sign}(M)$ for $|M| > 1$. Also the convective diffusion should remain positive when $M = 0$, while the pressure diffusion must be antisymmetric with respect to M. A simple choice is to take $f_1(M) = |M|$ and $f_2(M) = \text{sign}(M)$ for $|M| > 1$, and to introduce blending polynomials in M for $|M| < 1$ which merge smoothly into the supersonic segments. A quartic formula

$$f_1(M) = a_o + a_2 M^2 + a_4 M^4, \quad |M| < 1,$$

preserves continuity of f_1 and $\mathrm{d}f_1/\mathrm{d}M$ at $|M| = 1$ if

$$a_2 = \tfrac{3}{2} - 2a_o, \qquad a_4 = a_o - \tfrac{1}{2}.$$

Then a_o controls the diffusion at $M = 0$. For transonic flow calculations a good choice is $a_o = \frac{1}{4}$, while for very high speed flows it may be increased to $\frac{1}{2}$. A suitable blending formula for the pressure diffusion is

$$f_2(M) = \tfrac{1}{2} M(3 - M^2), \quad |M| < 1.$$

The diffusion corresponding to the convective terms is identical to the scalar diffusion of Jameson, Schmidt and Turkel [19], with a modification of the scaling, while the pressure term is the minimum modification needed to produce perfect upwinding in the supersonic zone. The scheme retains the property of the original scheme that it is compatible with constant stagnation enthalpy in steady flow. If one derives the viscosity corresponding to the flux splitting recently proposed by Liou and Steffen [23], following equation (7), one finds that their scheme produces first-order diffusion with a similar general form, and the present scheme may thus be regarded as a construction of artificial viscosity approximately equivalent to Liou–Steffen splitting.

2.7. Time-stepping schemes and multigrid

The discretization of the spatial derivatives reduces the partial differential equation to a semi-discrete equation which may be written in the form

$$\frac{\mathrm{d}w}{\mathrm{d}t} + R(w) = 0, \tag{16}$$

where w is the vector of flow variables at the mesh points, and $R(w)$ is the vector of the residuals, consisting of the flux balances augmented by the diffusive terms. In the case of a steady state calculation the details of the transient solution are immaterial, and the time-stepping scheme may be designed solely to maximize the rate of convergence.

If an explicit scheme is used, the permissible time step for stability may be so small that a very large number of time steps are needed to reach a steady state. This can be alleviated by using time steps of varying size in different locations, which are adjusted so that they are always close to the local stability limit. If the mesh interval increases with the distance from the body, the time step will also increase, producing an effect comparable to that of an increasing wave speed. Convergence to a steady state can be further accelerated by the use of a multigrid procedure of the type described below. With the aid of these measures explicit multistage schemes have proved extremely effective. Implicit schemes allow much larger time steps, but the work required in each time step may become excessively large, especially in three-dimensional calculations. In fact, it is suggested in the next section that a good way to construct efficient implicit schemes for calculating unsteady flows is to use an explicit multigrid scheme to solve the equations in each time step.

If one reduces the linear model problem corresponding to (16) to an ordinary differential equation by substituting a Fourier mode $\hat{w} = e^{ipx_j}$, the resulting Fourier symbol has an imaginary part proportional to the wave speed, and a negative real part proportional to the diffusion. Thus the time-stepping scheme should have a stability region which contains a substantial interval of the negative real axis, as well as an interval along the imaginary axis. To achieve this it pays to treat the convective and dissipative terms in a distinct fashion. Thus the residual is split as

$$R(w) = Q(w) + D(w),$$

where $Q(w)$ is the convective part and $D(w)$ the dissipative part. Denote the time level $n\Delta t$ by a superscript n. Then the multistage time-stepping scheme is formulated as

$$w^{(n+1,0)} = w^n,$$

$$\vdots$$

$$w^{(n+1,k)} = w^n - \alpha_k \Delta t\left(Q^{(k-1)} + D^{(k-1)}\right),$$

$$\vdots$$

$$w^{n+1} = w^{(n+1,m)},$$

where the superscript k denotes the kth stage, $\alpha_m = 1$, and

$$Q^{(0)} = Q(w^n), \qquad D^{(0)} = D(w^n),$$

$$\vdots$$

$$Q^{(k)} = Q\left(w^{(n+1,k)}\right),$$

$$D^{(k)} = \beta_k D\left(w^{(n+1,k)}\right) + (1-\beta_k) D^{(k-1)}.$$

The coefficients α_k are chosen to maximize the stability interval along the imaginary axis, and the coefficients β_k are chosen to increase the stability interval along the negative real axis.

Two schemes which have been found to be particularly effective are tabulated below. The first is a four-stage scheme with two evaluations of dissipation. Its coefficients are

$$\alpha_1 = \tfrac{1}{3}, \qquad \beta_1 = 1,$$
$$\alpha_2 = \tfrac{4}{15}, \qquad \beta_2 = \tfrac{1}{2},$$
$$\alpha_3 = \tfrac{5}{9}, \qquad \beta_3 = 0,$$
$$\alpha_4 = 1, \qquad \beta_4 = 0.$$

The second is a five-stage scheme with three evaluations of dissipation. Its coefficients are

$$\alpha_1 = \tfrac{1}{4}, \qquad \beta_1 = 1,$$
$$\alpha_2 = \tfrac{1}{6}, \qquad \beta_2 = 0,$$
$$\alpha_3 = \tfrac{3}{8}, \qquad \beta_3 = 0.56,$$
$$\alpha_4 = \tfrac{1}{2}, \qquad \beta_4 = 0,$$
$$\alpha_5 = 1, \qquad \beta_5 = 0.44.$$

The multigrid scheme is a full approximation scheme defined as follows [11,13]. Denote the grids by a subscript k. Start with a time step on the finest grid $k = 1$. Transfer the solution from a given grid to a coarser grid by a transfer operator $P_{k,k-1}$, so that the initial state on grid k is

$$w_k^{(0)} = P_{k,k-1} w_{k-1}.$$

Then on grid k the multistage time-stepping scheme is reformulated as

$$w_k^{(q+1)} = w_k^{(0)} - \alpha_n \Delta t \left(R_k^{(q)} + G_k \right),$$

where the residual $R_k^{(q)}$ is evaluated from current and previous values as above, and the forcing function G_k is defined as the difference between the aggregated residuals transferred from grid $k-1$ and the residual recalculated on grid k. Thus

$$G_k = Q_{k,k-1} R(w_{k-1}) - R\left(w_k^{(0)}\right),$$

where $Q_{k,k-1}$ is another transfer operator. On the first stage the forcing term G_k simply replaces the coarse grid residual by the aggregated fine grid residuals. The accumulated correction on a coarser grid is transferred to the next higher grid by an interpolation operator $I_{k-1,k}$ so that the solution on grid $k-1$ is updated by the formula

$$w_{k-1}^{\text{new}} = w_{k-1} + I_{k-1,k}\left(w_k - w_k^{(0)}\right).$$

The whole set of grids is traversed in a W-cycle in which time steps are only performed when moving down the cycle.

2.8. *Multigrid implicit scheme for unsteady flow*

Time-dependent calculations are needed for a number of important applications, such as flutter analysis, or the analysis of the flow past a helicopter rotor, in which the stability limit of

an explicit scheme forces the use of smaller time steps than would be needed for an accurate simulation. In this situation a multigrid explicit scheme can be used in an inner iteration to solve the equations of a fully implicit time-stepping scheme.

Suppose that (15) is approximated as

$$D_t w^{n+1} + R(w^{n+1}) = 0.$$

Here D_t is a kth-order accurate backward difference operator of the form

$$D_t = \frac{1}{\Delta t} \sum_{q=1}^{k} \frac{1}{q} (\Delta^-)^q,$$

where

$$\Delta^- w^{n+1} = w^{n+1} - w^n.$$

Applied to the linear differential equation

$$\frac{dw}{dt} = \alpha w,$$

the schemes with $k = 1,2$ are stable for all $\alpha \Delta t$ in the left half-plane (A-stable). Dahlquist has shown that A-stable linear multi-step schemes are at best second-order accurate [5]. Gear, however, has shown that the schemes with $k \leqslant 6$ are stiffly stable [7], and one of the higher-order schemes may offer a better compromise between accuracy and stability, depending on the application.

Equation (16) is now treated as a modified steady state problem to be solved by a multigrid scheme using variable local time steps in a fictitious time t^*. For example, in the case $k = 2$ one solves

$$\frac{\partial w}{\partial t^*} = R^*(w),$$

where

$$R^*(w) = \frac{3}{2\Delta t} w + R(w) + \frac{2}{\Delta t} w^n - \frac{1}{2\Delta t} w^{n-1},$$

and the last two terms are treated as fixed source terms. The first term shifts the Fourier symbol of the equivalent model problem to the left in the complex plane. While this promotes stability, it may also require a limit to be imposed on the magnitude of the local time step Δt^* relative to that of the implicit time step Δt. In the case of problems with moving boundaries the equations must be modified to allow for movement and deformation of the mesh.

This method has proved effective for the calculation of unsteady flows that might be associated with wing flutter [17]. It has the advantage that it can be added as an option to a computer program which uses an explicit multigrid scheme, allowing it to be used for the efficient calculation of both steady and unsteady flows.

2.9. Numerical results of multigrid calculations with upwind biasing

Figs. 3–7 display the results of multigrid calculations using the CUSP scheme with switched diffusion. Figs. 3–5 show transonic solutions for three different airfoils, calculated on a 160×32 mesh, and each of which is essentially converged in 12 multigrid cycles. The work in each cycle is about equal to two explicit time steps on the fine grid. It may be noted also that the computed drag coefficient of the Korn airfoil at the shock-free design point is zero to four digits. The drag coefficient is also computed to be zero to four digits for subsonic flows over a variety of airfoils with lift coefficients in the range up to 1.0. Very little change is observed between solutions calculated on 80×16 and 160×32 meshes, providing a further confirmation of accuracy.

The CUSP scheme produces very sharp shock waves in hypersonic flow, provided that care is taken to define the cell interface Mach number as the Mach number on the downwind side, so that downwind terms are perfectly cancelled in supersonic flow. This is illustrated in Figs. 6 and 7, which show the flow past a semicircular blunt body at Mach 8 and 20. It can be seen that quite rapid convergence, at a rate of the order of 0.9, continues to be obtained with the multigrid scheme in hypersonic flow.

Shock waves in transonic flow are less sharply resolved, but discrete shock waves with 2 or 3 interior points are obtained if the diffusion is scaled to a value somewhat less than that corresponding to full upwinding. Another way to achieve this is to use blending functions with the same asymptotic values for large Mach numbers, but smaller values when $M = 1$. One choice is

$$f_1(M) = \sqrt{\tfrac{1}{4} + M^2}\,\frac{\tfrac{1}{4} + M^2}{1 + M^2}, \qquad f_2(M) = \frac{M}{\sqrt{1 + M^2}}.$$

When very sharp resolution of weak shocks is required, the results can be improved by characteristic splitting with matrix diffusion using Roe averaging. Discrete shock waves with just one interior point are then obtained when flux-limited dissipation is used, following equation (9). The choice of limiter can significantly affect the accuracy. If the limiter is too stringent the lift is noticeably underpredicted even on a 320×64 mesh. For example, if one uses α-mean with $\alpha = 1$ the lift coefficient for the RAE 2822 airfoil at Mach 0.75 and 3° angle of attack is calculated on a 320×64 mesh to be 1.092, whereas with $\alpha = 2$ it is calculated to be 1.121. When the limiter is relaxed, on the other hand, it becomes progressively more difficult to achieve convergence to a steady state, and there is a tendency for convergence to stop at an error threshold in the region of 10^4. The switched scheme can produce equally perfect shocks in steady flow when it is combined with matrix diffusion, provided that the shocks are not too weak. When multigrid acceleration is introduced it also generally converges more rapidly to a steady state. Thus it may be preferred for steady state calculations, while flux-limited dissipation may be needed for perfect oscillation control in the calculation of unsteady flows.

Figs. 8–11 show the results of multigrid calculations on a 320×64 mesh for the NACA 0012 airfoil at Mach 0.85 and 1° angle of attack and the RAE 2822 airfoil at Mach 0.75 and 3° angle of attack. Characteristic splitting was used in all these calculations. The first pair of figures show results for the RAE 2822 airfoil calculated with the switched scheme, and with flux-limited

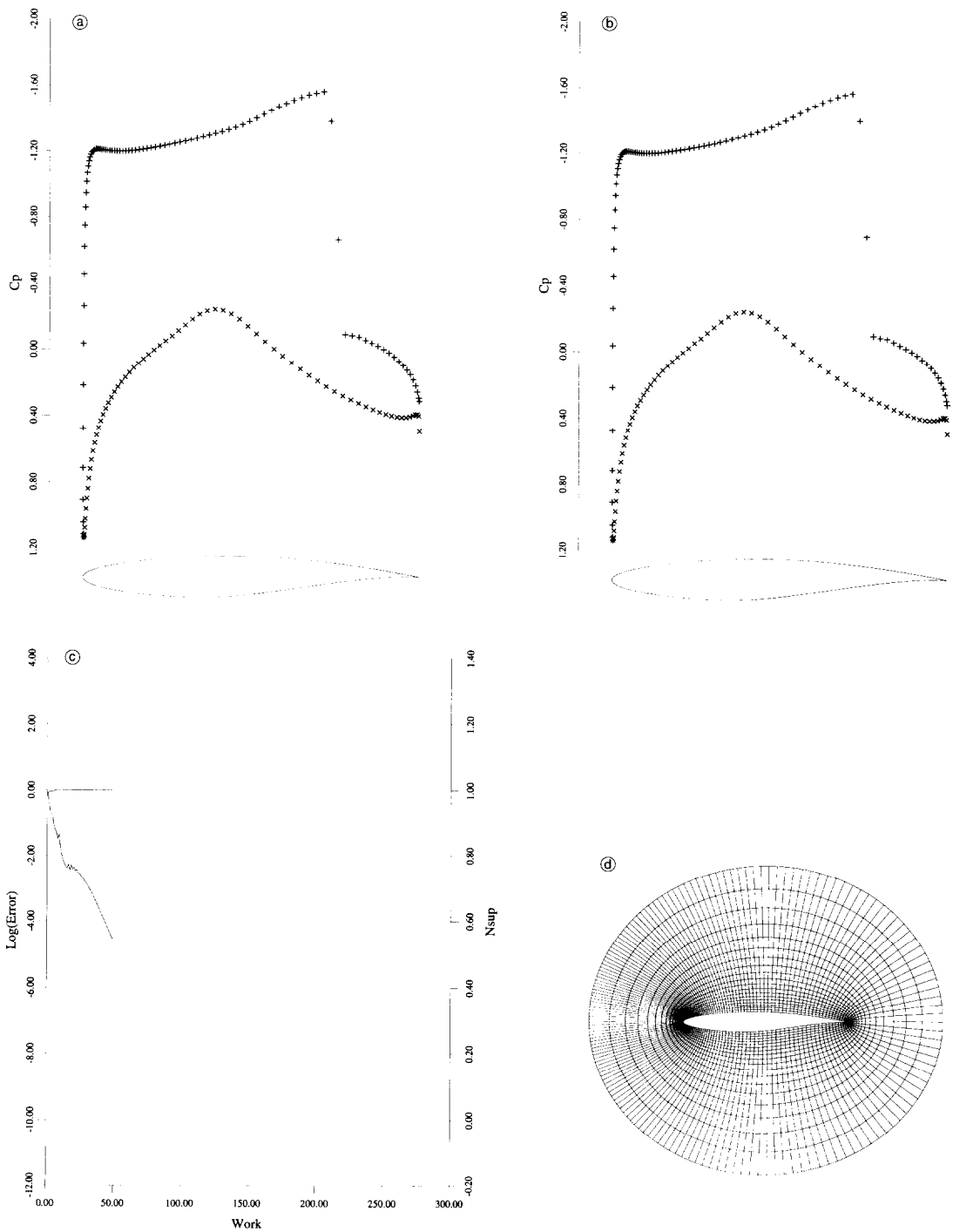

Fig. 3. RAE 2822. Mach 0.750, angle of attack 3°, 160×32 mesh. (a) C_p after 12 cycles. $C_l = 1.1262$ and $C_d = 0.0467$. (b) C_p after 50 cycles. $C_l = 1.1284$ and $C_d = 0.0470$. (c) Convergence. (d) Grid.

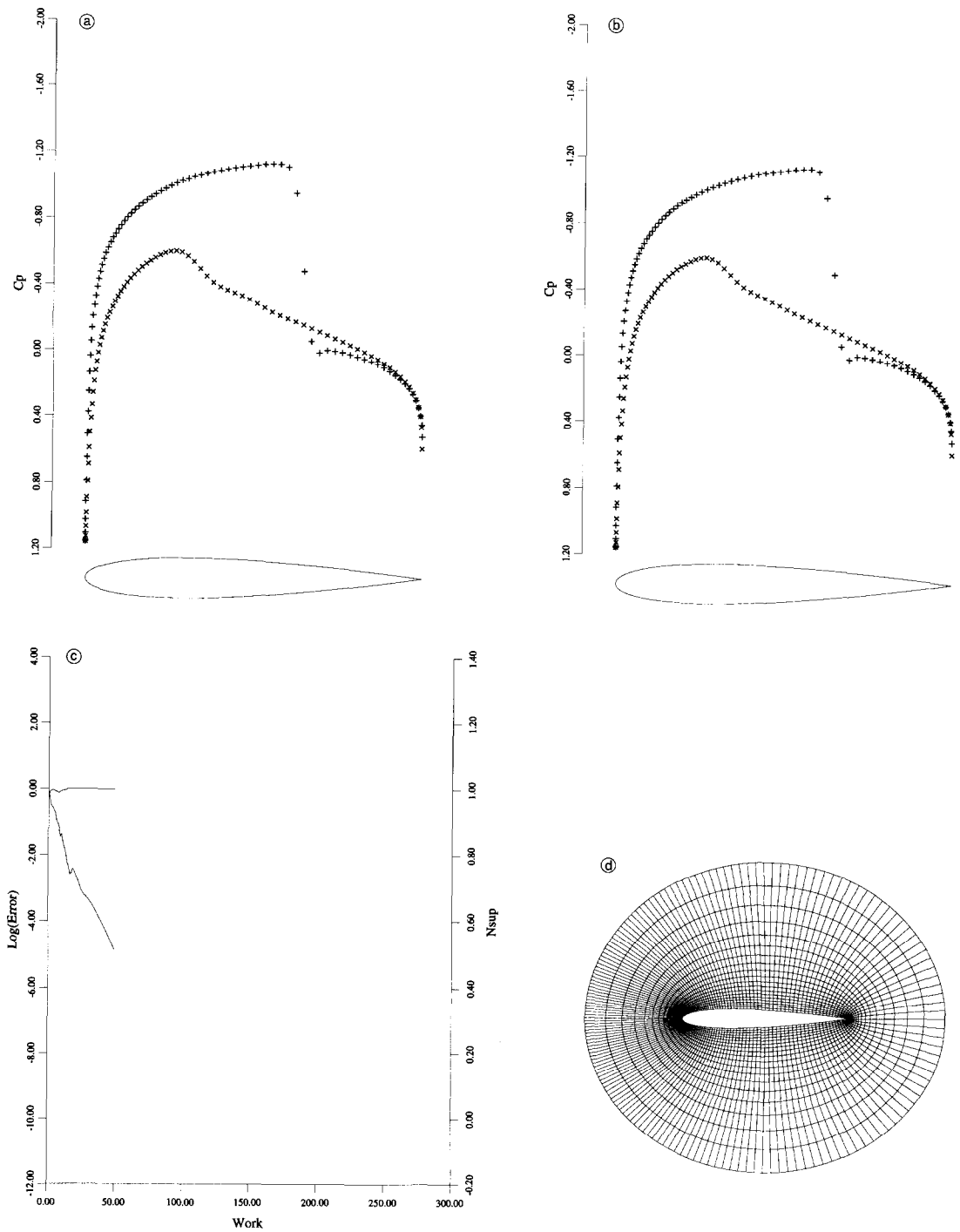

Fig. 4. NACA 0012. Mach 0.800, angle of attack 1.25°, 160×32 mesh. (a) C_p after 12 cycles. $C_l = 0.3653$ and $C_d = 0.0234$. (b) C_p after 50 cycles. $C_l = 0.3665$ and $C_d = 0.0234$. (c) Convergence. (d) Grid.

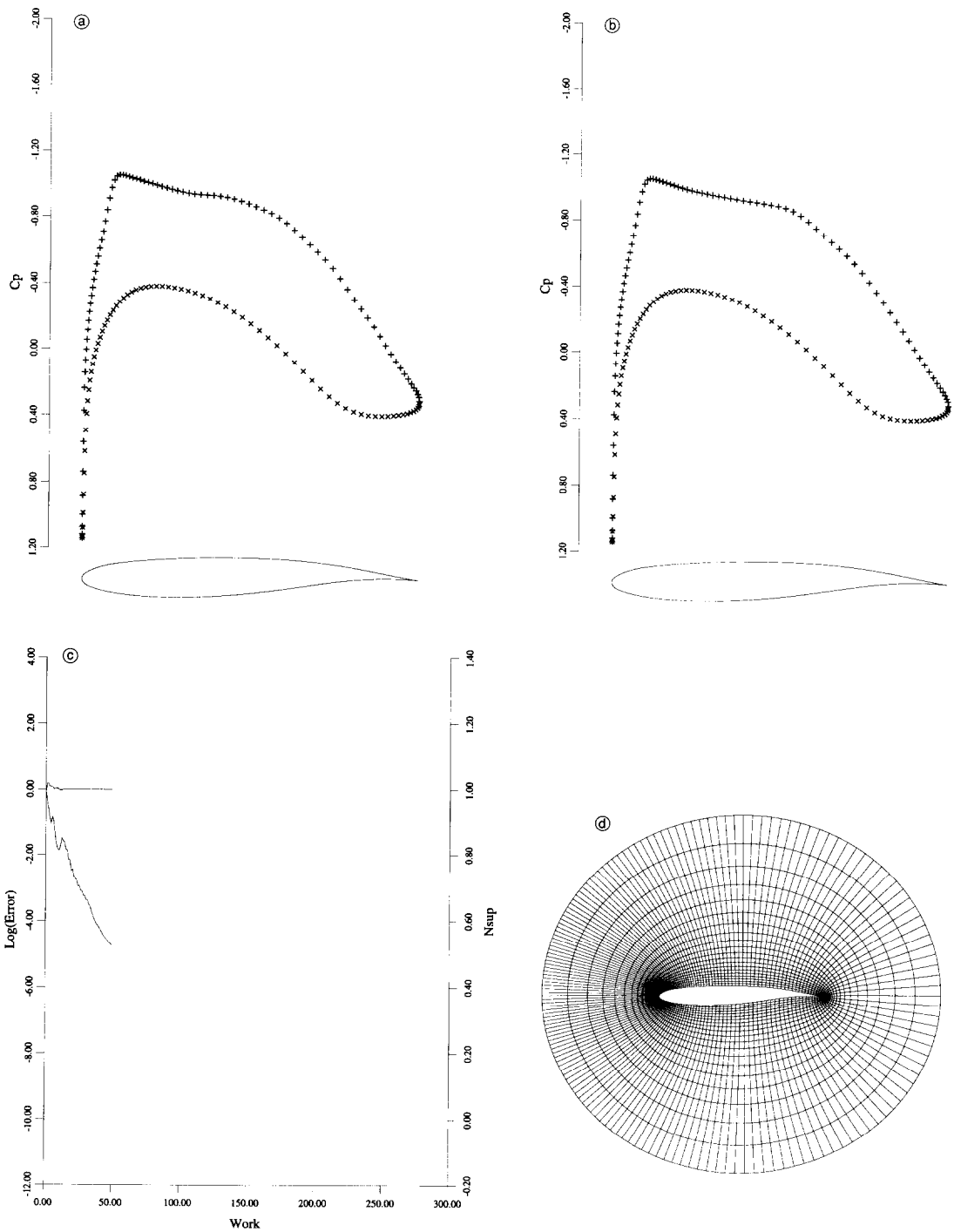

Fig. 5. KORN airfoil. Mach 0.750, angle of attack 0°, 160×32 mesh. (a) C_p after 12 cycles. $C_l = 0.6309$ and $C_d = 0.0001$. (b) C_p after 50 cycles. $C_l = 0.6311$ and $C_d = 0.000$. (c) Convergence. (d) Grid.

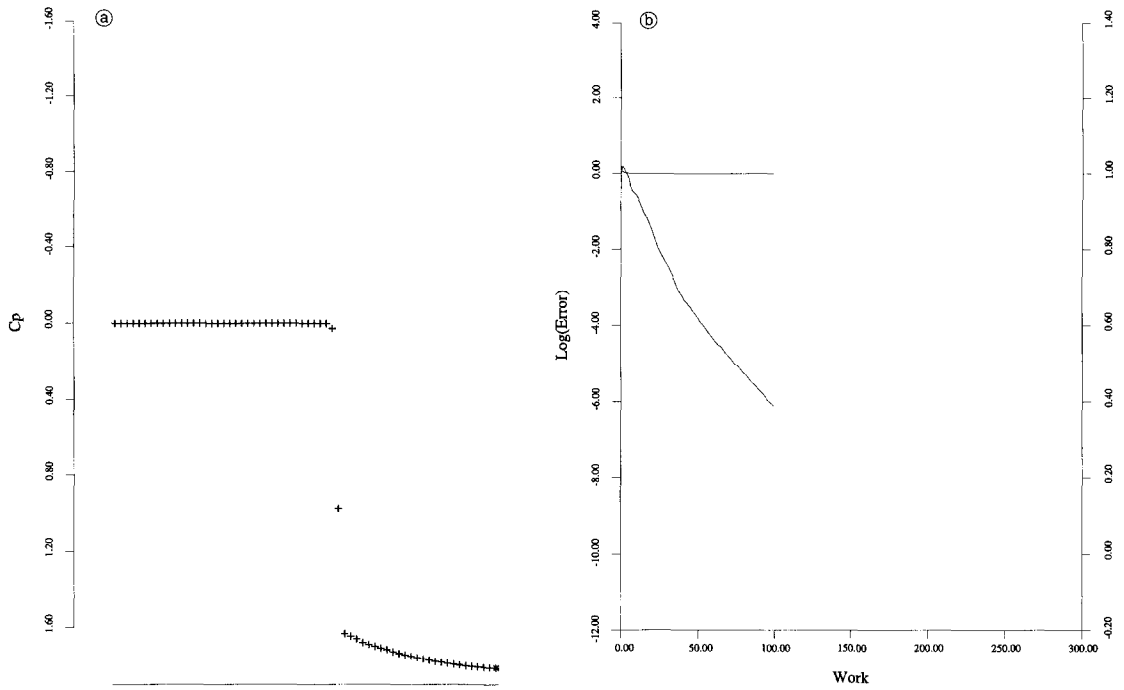

Fig. 6. Bluff body. Mach 8, 160×64 mesh. (a) C_p on the centerline in front of the body. (b) Convergence.

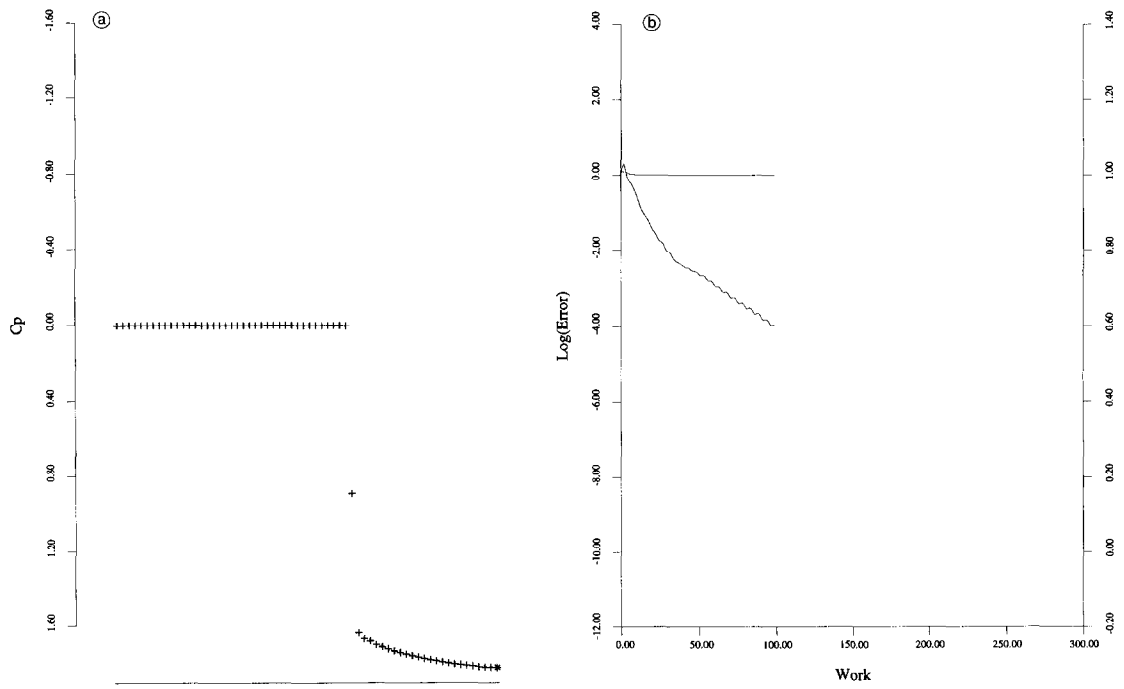

Fig. 7. Bluff body. Mach 20, 160×64 mesh. (a) C_p on the centerline in front of the body. (b) Convergence.

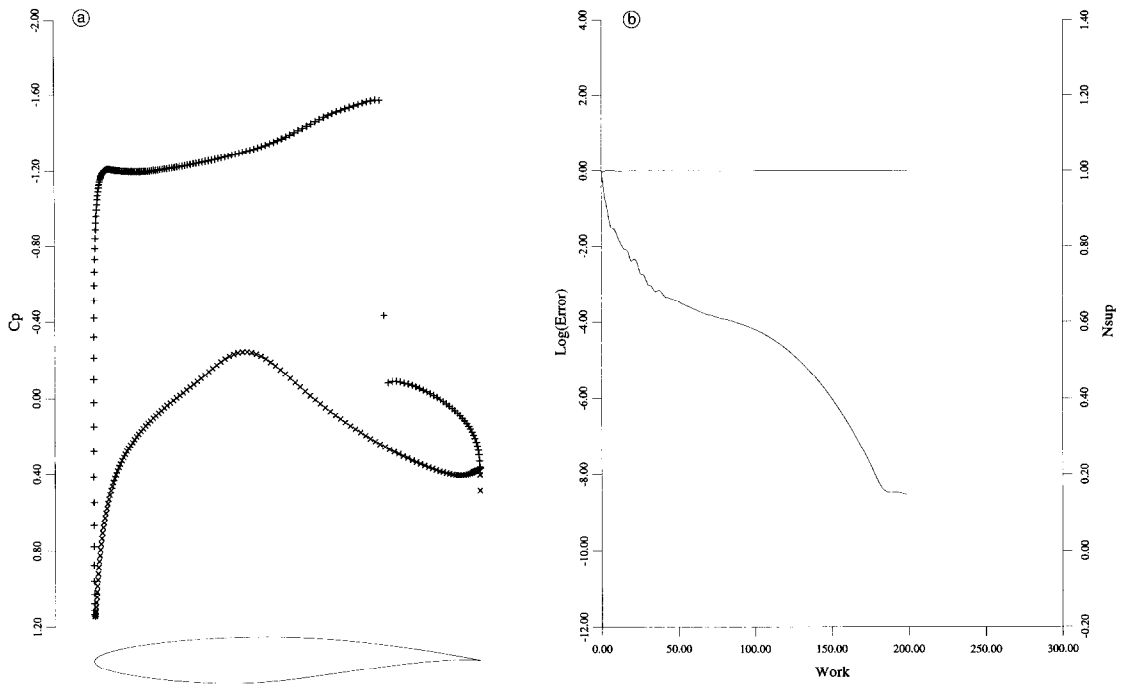

Fig. 8. RAE 2822 with switched matrix dissipation. Mach 0.750, angle of attack 3°, 320×64 mesh. (a) C_p. $C_l = 1.1167$ and $C_d = 0.0455$. (b) Convergence.

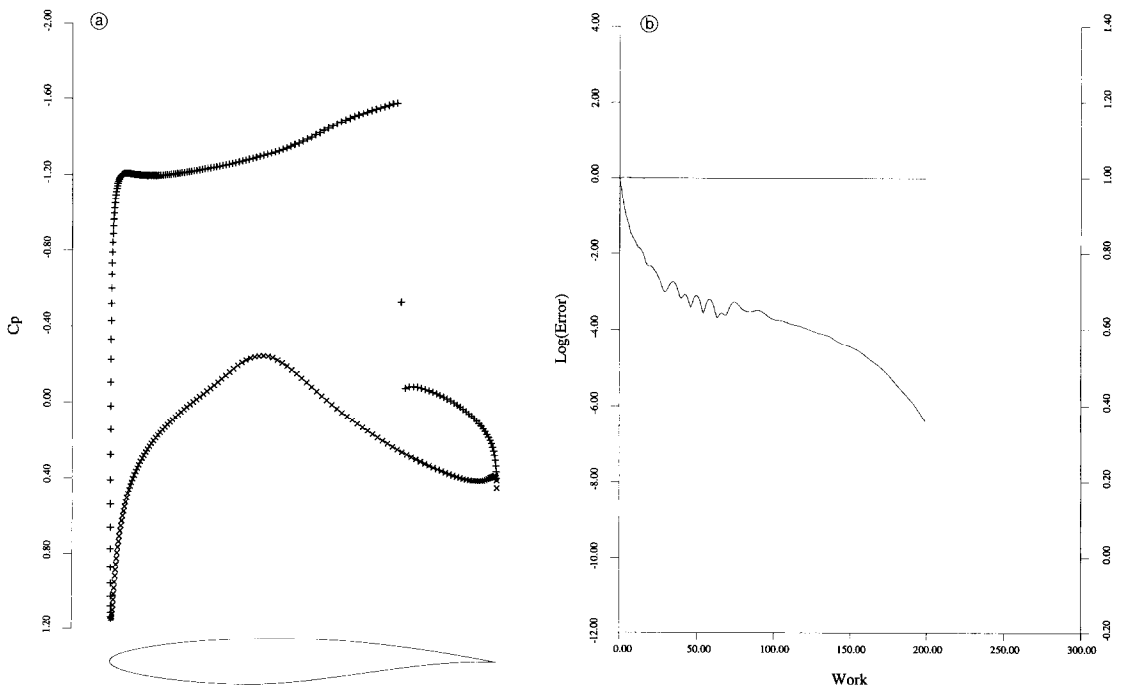

Fig. 9. RAE 2822 with flux-limited dissipation. Mach 0.750, angle of attack 3°, 320×64 mesh. (a) C_p. $C_l = 1.1194$ and $C_d = 0.0456$. (b) Convergence.

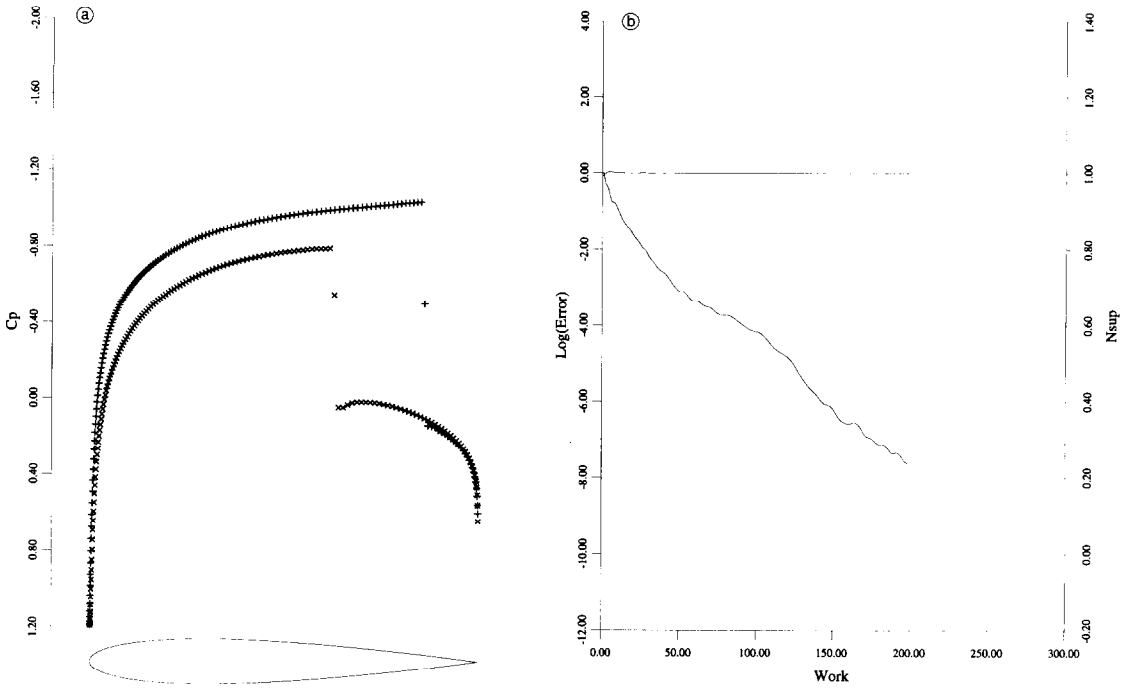

Fig. 10. NACA 0012 with switched matrix dissipation. Mach 0.850, angle of attack 1°, 320×64 mesh. (a) C_p. $C_l = 0.3729$ and $C_d = 0.0575$. (b) Convergence.

dissipation using α-mean with $\alpha = 1.5$. The second pair of figures show the same comparison for the NACA 0012 airfoil. The two schemes give more or less identical results, but the switched scheme converges faster. When the switched scheme is applied to the NACA 0012 airfoil at Mach 0.8 and 1.25° angle of attack, however, it does not resolve the very weak shock that appears on the lower surface as cleanly as the flux-limited dissipation. Characteristic splitting also produces perfectly resolved discrete shock waves in hypersonic flow, but the error in the stagnation enthalpy is substantial when the Mach number exceeds 8, finally becoming so large that the results may be unacceptable.

3. The design problem

3.1. Formulation as a control problem

Ultimately the designer seeks to optimize the geometric shape taking into account the trade-offs between aerodynamic performance, structure weight and the requirement for internal volume to contain fuel and payload. The subtlety and complexity of fluid flow is such that it is unlikely that repeated trials in an interactive analysis and design procedure can lead to a truly optimum design, unless the process is made automatic. Progress toward automatic design has been restricted by the extreme computing costs that might be incurred, but useful design

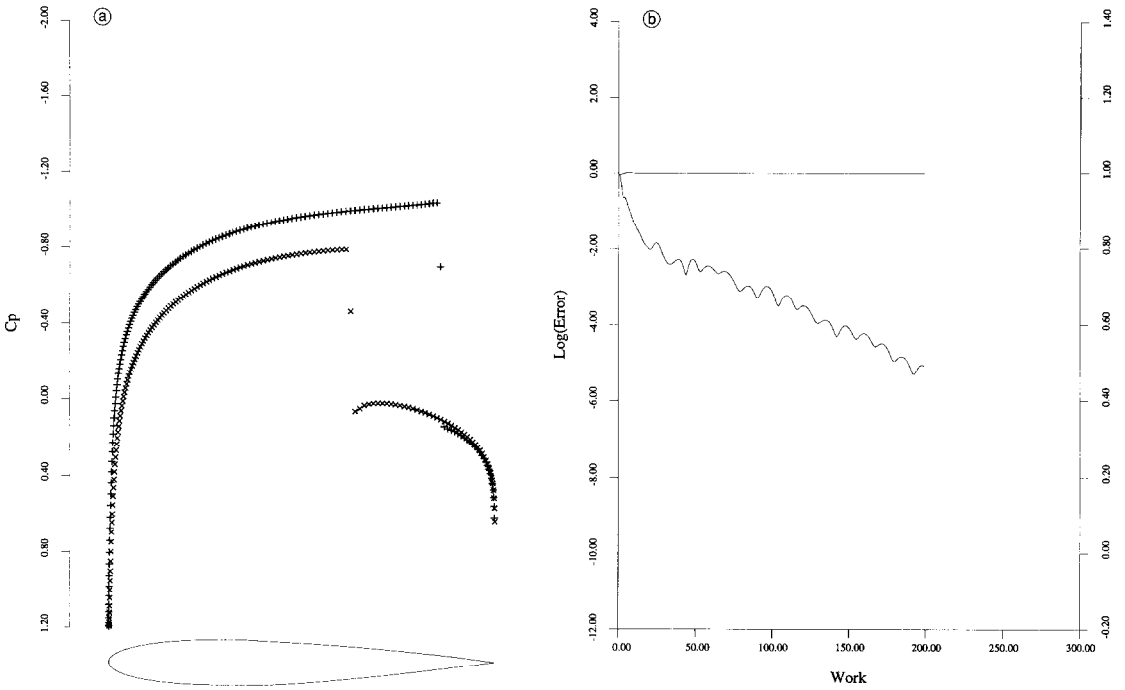

Fig. 11. NACA 0012 with flux-limited dissipation. Mach 0.850, angle of attack 1°, 320×64 mesh. (a) C_p. $C_l = 0.3768$ and $C_d = 0.0576$. (b) Convergence.

methods have been devised for various simplified cases, such as two-dimensional airfoils and cascades, and wings in potential flow. In particular, it has been recognized that the designer generally has an idea of the kind of pressure distribution that will lead to the desired performance. Thus it is useful to consider the inverse problem of calculating the shape that will lead to a given pressure distribution. Such a shape does not necessarily exist, unless the pressure distribution satisfies certain constraints, and the problem must therefore be very carefully formulated.

The problem of designing a two-dimensional profile to attain a desired pressure distribution was first studied by Lighthill, who solved it for the case of incompressible flow with a conformal mapping of the profile to a unit circle [21]. The speed over the profile is

$$q = \frac{1}{h}|\nabla\phi|,$$

where ϕ is the potential, which is known for incompressible flow, and h is the modulus of the mapping function. The surface value of h can be obtained by setting $q = q_{\mathrm{d}}$, where q_{d} is the desired speed, and since the mapping function is analytic, it is uniquely determined by the value of h on the boundary. A solution exists for a given speed q_∞ at infinity only if

$$\frac{1}{2\pi}\oint q \, \mathrm{d}\theta = q_\infty,$$

and there are additional constraints on q if the profile is required to be closed.

The difficulty that the objective may be unattainable can be circumvented by regarding the design problem as a control problem in which the control is the shape of the boundary. A variety of alternative formulations of the design problem can then be treated systematically within the framework of the mathematical theory for control of systems governed by partial differential equations [22]. Suppose that the boundary is defined by a function $f(\boldsymbol{x})$, where $\boldsymbol{x}$ is the position vector, and the desired objective is measured by a cost function I. This may, for example, measure the deviation from a desired surface pressure distribution, but it can also represent other measures of performance such as lift and drag. In any case, if the objective is unattainable, it is still possible to find a minimum of the cost function. Suppose that a variation δf in the control produces a variation δI in the cost. Following control theory, δI can be expressed to first order as an inner product

$$\delta I = (g, \delta f),$$

where the gradient g is independent of the particular variation δf, and can be determined by solving an adjoint equation. Now if one makes a shape change

$$\delta f = -\lambda g,$$

then

$$\delta I = -\lambda(g, g) < 0,$$

assuring a reduction in I. After making such a modification, the gradient can be recalculated and the process repeated to follow a path of steepest descent until a minimum is reached. In order to avoid violating constraints, such as a minimum acceptable wing thickness, the gradient may be projected into the allowable subspace within which changes are permitted in the control function. In this way one can devise procedures which must necessarily converge at least to a local minimum, and which can be accelerated by the use of more sophisticated descent methods such as the conjugate gradient algorithm. There is the possibility of more than one local minimum, but in any case the method will lead to an improvement over the original design.

The application of control theory to optimal aerodynamic shape design has been explored by the author [15,16]. The next section presents the formulation for the case of airfoils in transonic flow. The governing equation is taken to be the transonic potential flow equation, and the profile is generated by conformal mapping from a unit circle. Thus the control is taken to be the modulus of the mapping function on the boundary. This leads to a generalization of Lighthill's method both to compressible flow and to design for more general criteria. Numerical results are presented in Section 3.3. The mathematical development resembles, in certain respects, the method of calculating transonic potential flow developed by Bristeau, Pironneau, Glowinski, Périaux, Perrier and Poirier, who reformulated the solution of the flow equations as a least squares problem in control theory [3]. Pironneau has also studied the use of control theory for optimum shape design of systems governed by elliptic equations [25].

3.2. Design for potential flow using conformal mapping

Consider the case of two-dimensional compressible inviscid flow. In the absence of shock waves, an initially irrotational flow will remain irrotational, and we can assume that the velocity vector $\boldsymbol{q}$ is the gradient of a potential ϕ. In the presence of weak shock waves this remains a fairly good approximation.

Let p, ρ, c, and M be the pressure, density, speed of sound, and Mach number q/c. Then the potential flow equation is

$$\nabla \cdot (\rho \nabla \phi) = 0, \tag{17}$$

where the density is given by

$$\rho = \left\{1 + \tfrac{1}{2}(\gamma - 1)M_\infty^2(1 - q^2)\right\}^{1/(\gamma-1)}, \tag{18}$$

while

$$p = \frac{\rho^\gamma}{\gamma M_\infty^2}, \qquad c^2 = \frac{\gamma p}{\rho}. \tag{19}$$

Here M_∞ is the Mach number in the free stream, and the units have been chosen so that p and q have the value unity in the far field.

Suppose that the domain D exterior to the profile C in the z-plane is conformally mapped onto the domain exterior to a unit circle in the σ-plane as sketched in Fig. 12. Let R and θ be polar coordinates in the σ-plane, and let r be the inverted radial coordinate $1/R$. Also let h be the modulus of the derivative of the mapping function

$$h = \left|\frac{\mathrm{d}z}{\mathrm{d}\sigma}\right|. \tag{20}$$

Now the potential flow equation becomes

$$\frac{\partial}{\partial \theta}(\rho \phi_\theta) + r\frac{\partial}{\partial r}(r\rho\phi_r) = 0 \quad \text{in } D, \tag{21}$$

where the density is given by equation (18), and the circumferential and radial velocity components are

$$u = \frac{r\phi_\theta}{h}, \qquad v = \frac{r^2\theta_r}{h}, \tag{22}$$

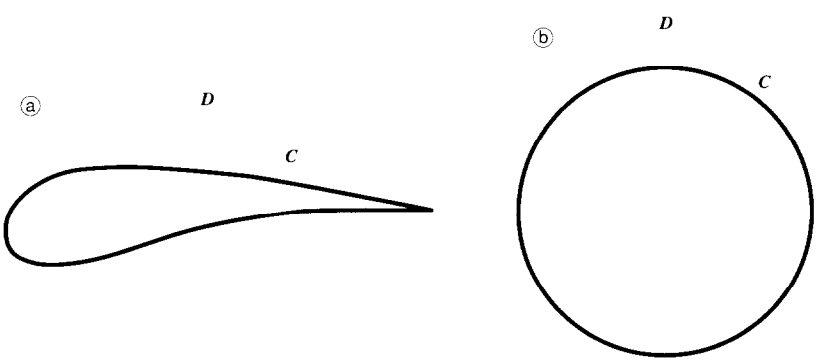

Fig. 12. Conformal mapping. (a) z-plane. (b) σ-plane.

while

$$q^2 = u^2 + v^2. \tag{23}$$

The condition of flow tangency leads to the Neumann boundary condition

$$v = \frac{1}{h}\frac{\partial \phi}{\partial r} = 0 \quad \text{on } C. \tag{24}$$

In the far field, the potential is given by an asymptotic estimate, leading to a Dirichlet boundary condition at $r = 0$ [9].

Suppose that it is desired to achieve a specified velocity distribution q_d on C. Introduce the cost function

$$I = \frac{1}{2}\int_C (q - q_d)^2 \, d\theta.$$

The design problem is now treated as a control problem where the control function is the mapping modulus h, which is to be chosen to minimize I subject to the constraints defined by the flow equations (17)–(24).

A modification δh to the mapping modulus will result in variations $\delta\phi$, δu, δv, and $\delta\rho$ to the potential, velocity components, and density. The resulting variation in the cost will be

$$\delta I = \int_C (q - q_d)\delta q \, d\theta, \tag{25}$$

where, on C, $q = u$. Also,

$$\delta u = r\frac{\delta\phi_\theta}{h} - u\frac{\delta h}{h}, \qquad \delta v = r^2\frac{\delta\phi_r}{h} - v\frac{\delta h}{h},$$

while according to equation (18)

$$\frac{\partial \rho}{\partial u} = -\frac{\rho u}{c^2}, \qquad \frac{\partial \rho}{\partial v} = -\frac{\rho v}{c^2}.$$

It follows that $\delta\phi$ satisfies

$$L\delta\phi = -\frac{\partial}{\partial\theta}\left(\rho M^2\phi_\theta\frac{\delta h}{h}\right) - r\frac{\partial}{\partial r}\left(\rho M^2 r\phi_r\frac{\delta h}{h}\right),$$

where

$$L \equiv \frac{\partial}{\partial\theta}\left\{\rho\left(1 - \frac{u^2}{c^2}\right)\frac{\partial}{\partial\theta} - \frac{\rho uv}{c^2}r\frac{\partial}{\partial r}\right\} + r\frac{\partial}{\partial r}\left\{\rho\left(1 - \frac{v^2}{c^2}\right)r\frac{\partial}{\partial r} - \frac{\rho uv}{c^2}\frac{\partial}{\partial\theta}\right\}. \tag{26}$$

Then, if ψ is any periodic differentiable function which vanishes in the far field,

$$\int_D \frac{\psi}{r^2} L\,\delta\phi \, dS = \int_D \rho M^2 \nabla\phi\cdot\nabla\psi\frac{\delta h}{h} dS, \tag{27}$$

where dS is the area elment $r\,dr\,d\theta$, and the right-hand side has been integrated by parts.

Now we can augment equation (25) by subtracting the constraint (27). The auxiliary function ψ then plays the role of a Lagrange multiplier. Thus

$$\delta I = \int_C (q - q_d) q \frac{\delta h}{h} d\theta - \int_C \delta\phi \frac{\partial}{\partial\theta}\left(\frac{q - q_d}{h}\right) d\theta$$
$$- \int_D \frac{\psi}{r^2} L\delta\psi \, dS + \int_D \rho M^2 \nabla\phi \cdot \nabla\psi \frac{\delta h}{h} dS.$$

Now suppose that ψ satisfies the adjoint equation

$$L\psi = 0 \quad \text{in } D \tag{28}$$

with the boundary condition

$$\frac{\partial\psi}{\partial r} = \frac{1}{\rho}\frac{\partial}{\partial\theta}\left(\frac{q - q_d}{h}\right) \quad \text{on } C. \tag{29}$$

Then, integrating by parts,

$$\int_D \frac{\psi}{r^2} L \, \delta\phi \, dS = -\int_C \rho\psi_r \, \delta\phi \, d\theta$$

and

$$\delta I = -\int_C (q - q_d) q \frac{\delta h}{h} d\theta + \int_D \rho M^2 \nabla\phi \cdot \nabla\psi \frac{\delta h}{h} dS. \tag{30}$$

Here the first term represents the direct effect of the change in the metric, while the area integral represents a correction for the effect of compressibility.

Equation (30) can be further simplified to represent δI purely as a boundary integral because the mapping function is fully determined by the value of its modulus on the boundary. Set

$$\log \frac{dz}{d\sigma} = f + i\beta,$$

where

$$f = \log\left|\frac{dz}{d\sigma}\right| = \log h$$

and

$$\delta f = \frac{\delta h}{h}.$$

Then f satisfies Laplace's equation

$$\Delta f = 0 \quad \text{in } D$$

and, if there is no stretching in the far field, $f \to 0$. Also δf satisfies the same condition. Introduce another auxiliary function P which satisfies

$$\Delta P = \rho M^2 \nabla\psi \cdot \nabla\psi \quad \text{in } D \tag{31}$$

and

$$P = 0 \quad \text{on } C.$$

Then, the area integral in equation (30) is

$$\int_D \Delta P \, \delta f \, \mathrm{d}S = \int_C \delta f \frac{\partial P}{\partial r} \mathrm{d}\theta - \int_D P \Delta \delta f \, \mathrm{d}S,$$

and finally

$$\delta I = \int_C g \, \delta f \, \mathrm{d}\theta,$$

where

$$g = \frac{\partial P}{\partial r} - (q - q_\mathrm{d})q. \tag{32}$$

This suggest setting

$$\delta f = -\lambda g,$$

so that, if λ is a sufficiently small positive quantity,

$$\delta I = -\int_C \lambda g^2 \, \mathrm{d}\theta < 0.$$

Arbitrary variations in δf cannot, however, be admitted. The condition that $f \to 0$ in the far field, and also the requirement that the profile should be closed, imply constraints which must be satisfied by f on the boundary C. Suppose that $\log(\mathrm{d}z/\mathrm{d}\sigma)$ is expanded as a power series

$$\log\left(\frac{\mathrm{d}z}{\mathrm{d}\sigma}\right) = \sum_{n=0}^{\infty} \frac{c_n}{\sigma^n} \tag{33}$$

where only negative powers are retained, because otherwise $(\mathrm{d}z/\mathrm{d}\sigma)$ would become unbounded for large σ. The condition that $f \to 0$ as $\sigma \to \infty$ implies

$$c_0 = 0.$$

Also, the change in z on integration around a circuit is

$$\Delta z = \int \frac{\mathrm{d}z}{\mathrm{d}\sigma} \mathrm{d}\sigma = 2\pi i c_1,$$

so the profile will be closed only if

$$c_1 = 0.$$

In order to satisfy these constraints, we can project g onto the admissible subspace for f by setting

$$c_0 = c_1 = 0. \tag{34}$$

Then the projected gradient $\tilde{g}$ is orthogonal to $g - \tilde{g}$ and, if we take

$$\delta f = -\lambda \tilde{g},$$

it follows that to first order

$$\delta I = -\lambda \int_C g\tilde{g}\, d\theta = -\lambda \int_C (\tilde{g} + g - \tilde{g}) g\, d\theta = -\lambda \int_C \tilde{g}^2\, d\theta < 0.$$

If the flow is subsonic, this procedure should converge toward the desired speed distribution since the solution will remain smooth, and no unbounded derivatives will appear. If, however, the flow is transonic, one must allow for the appearance of shock waves in the trial solutions, even if q_d is smooth. Then $q - q_d$ is not differentiable. This difficulty can be circumvented by a more sophisticated choice of the cost function. Consider the choice

$$I = \frac{1}{2} \int_C \left(\lambda_1 S^2 + \lambda_2 \left(\frac{dS}{d\theta} \right)^2 \right) d\theta,$$

where λ_1 and λ_2 are parameters, and the periodic function $S(\theta)$ satisfies the equation

$$\lambda_1 S - \lambda_2 \frac{d^2 S}{d\theta^2} = q - q_d. \tag{35}$$

Then,

$$\begin{aligned} \delta I &= \int_C \left(\lambda_1 S\, \delta S + \lambda_2 \frac{dS}{d\theta} \frac{d}{d\theta} \delta S \right) d\theta \\ &= \int_C S \left(\lambda_1\, \delta S - \lambda_2 \frac{d^2}{d\theta^2} \delta S \right) d\theta \\ &= \int_C S\, \delta q\, d\theta. \end{aligned}$$

Thus, S replaces $q - q_d$ in the previous formulas, and if one modifies the boundary condition (29) to

$$\frac{\partial \psi}{\partial r} = \frac{1}{\rho} \frac{\partial}{\partial \theta} \left(\frac{S}{h} \right) \quad \text{on } C \tag{36}$$

the formula for the gradient becomes

$$g = \frac{\partial P}{\partial r} - Sq$$

instead of equation (32). Smoothing can also be introduced directly in the descent procedure by choosing δf to satisfy

$$\delta f - \frac{\partial}{\partial\theta}\beta\frac{\partial}{\partial\theta}\delta f - \lambda g, \tag{37}$$

where β is a smoothing parameter. Then to first order

$$\int g\ \delta f = -\frac{1}{\lambda}\int\left(\delta f^2 - \delta f\frac{\partial}{\partial\theta}\beta\frac{\partial}{\partial\theta}\delta f\right)\mathrm{d}\theta$$

$$= -\frac{1}{\lambda}\int\left(\delta f^2 + \beta\left(\frac{\partial}{\partial\theta}\delta f\right)^2\right)\mathrm{d}\theta < 0.$$

The final design procedure is thus as follows. Choose an initial profile and corresponding mapping function f. Then:

Step 1. Solve the flow equations (17)–(24) for ϕ, u, v, q, and ρ.
Step 2. Solve the ordinary differential equation (35) for S.
Step 3. Solve the adjoint equation ((26) and (28)) or ψ subject to the boundary condition (36).
Step 4. Solve the auxiliary Poisson equation (31) for P.
Step 5. Evaluate

$$g = \frac{\partial P}{\partial r} - Sq$$

on C, and find its projection $\tilde{g}$ onto the admissible subspace of variations according to equation (34).

Step 6. Correct the boundary mapping function f_c by δf calculated from equation ((33) and (37))

$$\delta f = -\lambda\tilde{g}.$$

Step 7. Return to Step 1.

3.3. Numerical tests of optimal design

The practical realization of the design procedure depends on the availability of sufficiently fast and accurate numerical procedures for the implementation of the essential steps, in particular the solution of both the flow and the adjoint equations. If the numerical procedures are not accurate enough, the resulting errors in the gradient may impair or prevent the convergence of the descent procedure. If the procedures are too slow, the cumulative computing time may become excessive. In this case, it was possible to build the design procedure around the author's computer program FLO36, which solves the transonic potential flow equation in conservation form in a domain mapped to the unit disk. The solution is obtained by a very rapid multigrid alternating direction method. The original scheme is described in [10].

The program has been much improved since it was originally developed, and well-converged solutions of transonic flows on a mesh with 128 cells in the circumferential direction and 32 cells in the radial direction are typically obtained in 5–20 multigrid cycles. The scheme uses artificial dissipative terms to introduce upwind biasing which simulates the rotated difference scheme [9], while preserving the conservation form. The alternating direction method is a generalization of conventional alternating direction methods, in which the scalar parameters are replaced by upwind difference operators to produce a scheme which remains stable when the type changes from elliptic to hyperbolic as the flow becomes locally supersonic [10]. The conformal mapping is generated by a power series of the form of equation (33) with an additional term

$$\left(1-\frac{\varepsilon}{\phi}\right)\log\left(1-\frac{1}{\sigma}\right)$$

to allow for a wedge angle ε at the trailing edge. The coefficients are determined by an iterative process with the aid of fast Fourier transforms [9].

The adjoint equation has a form very similar to the flow equation. While it is linear in its dependent variable, it also changes type from elliptic in subsonic zones of the flow to hyperbolic in supersonic zones of the flow. Thus, it was possible to adapt exactly the same algorithm to solve both the adjoint and the flow equations, but with reverse biasing of the difference operators in the downwind direction in the adjoint equation, corresponding to the reversed direction of the zone of dependence. The Poisson equation (31) is solved by the Buneman algorithm.

An alternative procedure would be to derive the exact adjoint equation corresponding to the discrete equations which approximate the potential flow equation. This would produce the exact derivative of the discrete cost function with respect to the discrete control, at the expense of very complicated formulas and a costly inversion procedure. Numerical experiments confirm that in practice the scheme converges quite well when the flow and adjoint equations are discretized separately.

As an example of the application of the method, Fig. 13 presents a calculation in which an airfoil was redesigned to improve its transonic performance by reducing the pressure drag induced by the appearance of a shock wave. The drag coefficient was therefore included in the cost function so that equation (26) is replaced by

$$I=\frac{1}{2}\int_C\left(\lambda_1 S^2+\lambda_2\left(\frac{\mathrm{d}S}{\mathrm{d}\theta}\right)^2\right)\mathrm{d}\theta+\lambda_3 C_d,$$

where λ_3 is a parameter which may be varied to alter the trade-off between drag reduction and deviation from the desired pressure distribution. Representing the drag as

$$D=\int_C(p-p_\infty)\frac{\mathrm{d}y}{\mathrm{d}\theta}\,\mathrm{d}\theta$$

the procedure of Section 3.2 may be used to determine the gradient by solving the adjoint equation with a modified boundary condition. A penalty on the desired pressure distribution is

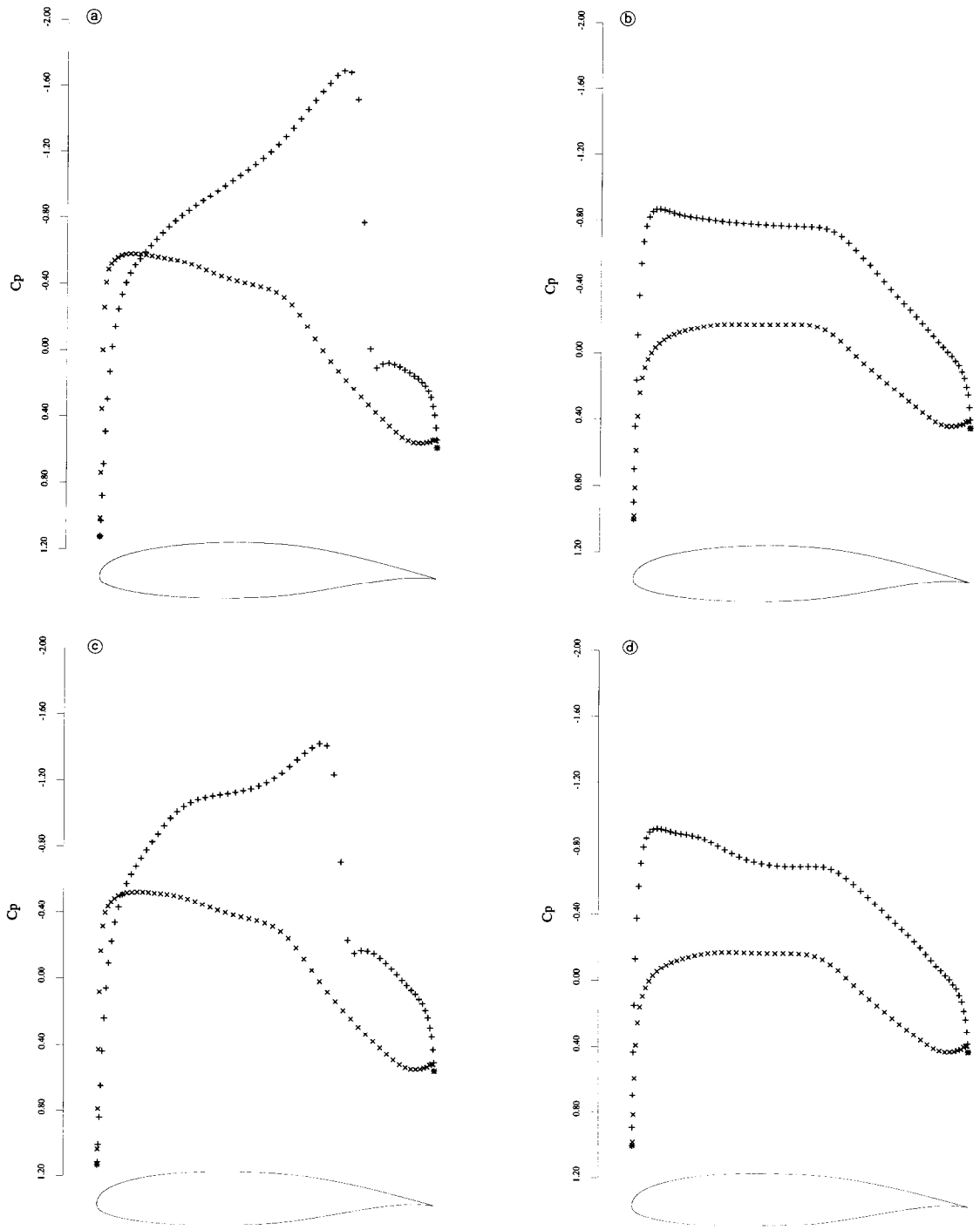

Fig. 13. Optimization of an airfoil at two design points. (a) C_p after zero design cycles. Design Mach 0.72, $C_l = 0.5982$, and $C_d = 0.0191$. (b) C_p after zero design cycles. Design Mach 0.2, $C_l = 0.5998$, and $C_d = -0.0001$. (c) C_p after two design cycles. Design Mach 0.72, $C_l = 0.5999$, and $C_d = 0.0057$. (d) C_p after two design cycles. Design Mach 0.2, $C_l = 0.5998$, and $C_d = -0.0001$.

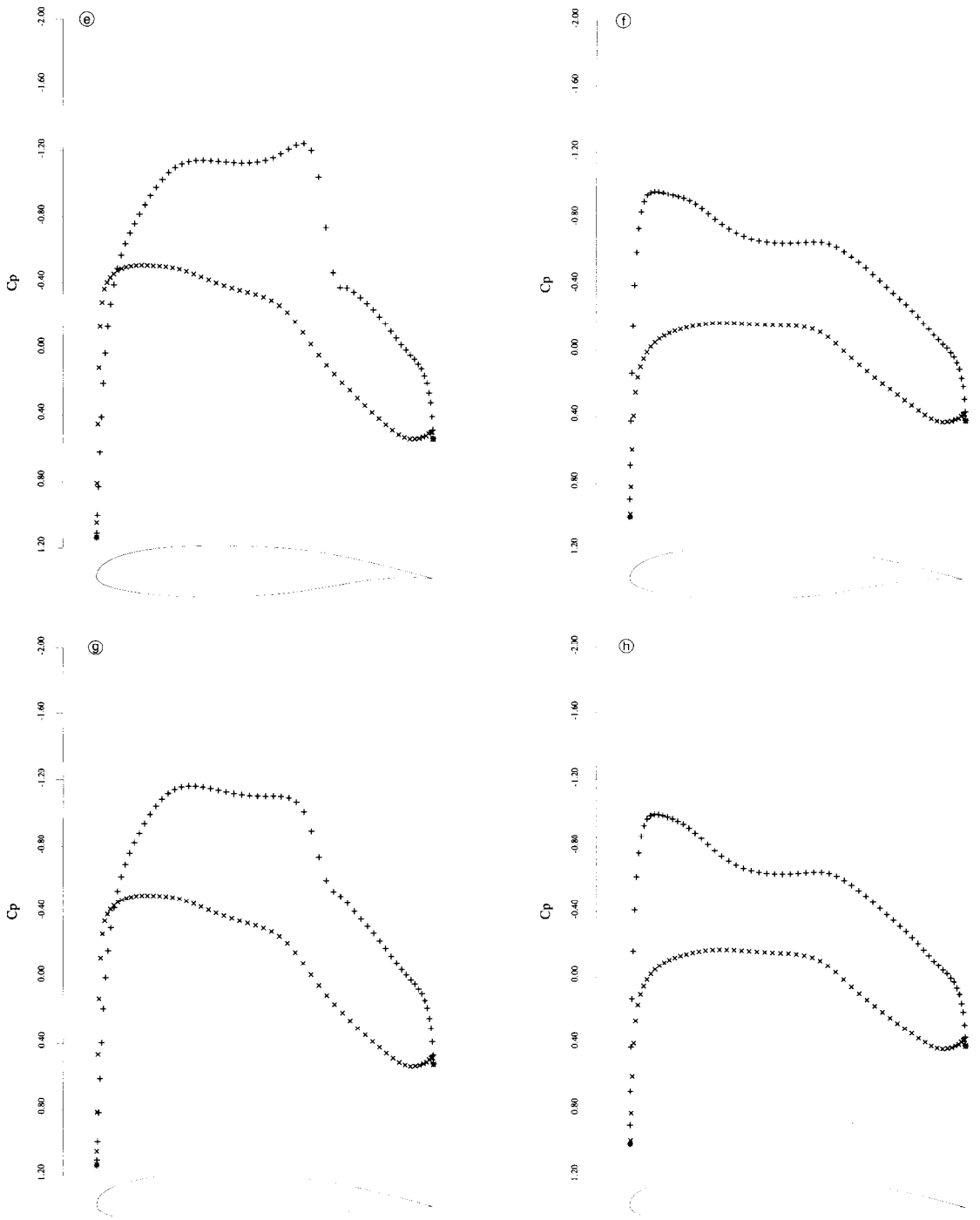

Fig. 13 (Continued). (e) C_p after four design cycles. Design Mach 0.72, $C_l = 0.6001$, and $C_d = 0.0015$. (f) C_p after four design cycles. Design Mach 0.2, $C_l = 0.5998$, and $C_d = -0.0001$. (g) C_p after six design cycles. Design Mach 0.72, $C_l = 0.6000$, and $C_d = 0.0003$. (h) C_p after six design cycles. Design Mach 0.2, $C_l = 0.5998$, and $C_d = -0.0001$.

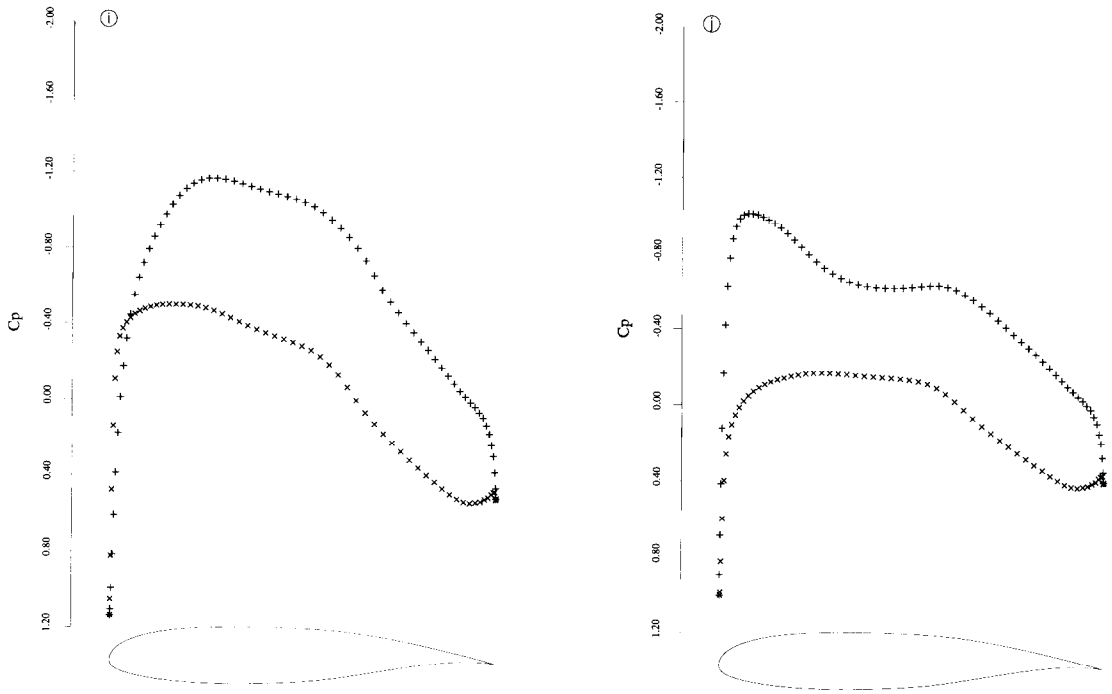

Fig. 13 (Continued). (i) C_p after eight design cycles. Design Mach 0.72, $C_l = 0.5999$, and $C_d = 0.0001$. (j) C_p after eight design cycles. Design Mach 0.2, $C_l = 0.5998$, and $C_d = -0.0001$.

still needed to avoid a situation in which the optimum shape is a flat plate with no lift and no drag.

It was also desired to preserve the subsonic characteristics of the airfoil. Therefore two design points were specified, Mach 0.20 and Mach 0.720, and in each case the lift coefficient was forced to be 0.6. The composite cost function was taken to be the sum of the values of the cost function at the two design points. The transonic drag coefficient was reduced from 0.0191 to 0.0001 in eight design cycles. In order to achieve this reduction the airfoil had to be modified so that its subsonic pressure distribution became more peaky at the leading edge. This is consistent with the results of experimental research on transonic airfoils, in which it has generally been found necessary to have a peaky subsonic pressure distribution in order to delay the onset of the transonic drag rise. It is also important to control the adverse pressure gradient on the rear upper surface, which can lead to premature separation of the viscous boundary layer. It can be seen that there is no steepening of this gradient due to the redesign.

4. Conclusion

The research presented here is directed toward some of the elements needed to produce computational tools for aerodynamic analysis that can meet the needs of aircraft design. Computational aerodynamics has now reached a plateau in which the basic framework for the

treatment of inviscid compressible flow is quite well established. It is known how to construct non-oscillatory schemes which capture shock waves and contact discontinuities with high resolution. Multigrid acceleration procedures can be used to produce rapidly convergent schemes for steady state calculations. Complex geometries can be treated with unstructured tetrahedral meshes, or alternatively with structured multi-block meshes in which separately generated component meshes are either patched or overlapped. Accuracy can be improved by automatic procedures for adaptive mesh refinement.

While it remains a formidable task to develop robust and reliable computer programs which incorporate all of these desirable features, well tested software incorporating some of them is now widely available. Rapid advances in computer technology have drastically reduced computational costs. Fig. 14 presents a solution of the Euler equations for the inviscid compressible flow past a complete aircraft, with flow through the engine ducts, which was computed on an IBM RISC 530 workstation. The figure displays color contours representing the surface pressure and Mach number distribution. The discrete solution was calculated on a mesh with 644,941 nodes and 3,961,024 tetrahedrons in 52 hours. Workstations which are at least five times faster that the RISC 530 will be available in the very near future. Thus, it will be possible to perform calculations of this magnitude in an environment of distributed computing, in which small design groups control their own computing resources, and access to larger scale remote facilities will only be needed for occasional calculations.

In situations where the aerodynamic design requires the analysis of flows in which the viscous effects are secondary, currently available computer methods are quite adequate, and the computational costs are low enough to permit them to be used routinely. This is the case, for example, for the analysis of long range aircraft in their cruising condition. The analysis of flows dominated by viscous effects, such as would be needed, for example, to predict the maximum lift of a wing before it stalls, presents a far more severe problem. This is due both to the disparity of scales between the viscous dominated regions and the global flow, and the complexity which results from the onset of turbulence at the very high Reynolds numbers associated with full scale flight, of the order of 30 million. Given that the complexity of a computation which resolves the smallest scale eddies in both space and time is proportional to the cube of the Reynolds number, it is not feasible to perform direct simulations of complex flow.

Even if the small scale motions are eliminated from the analysis by Reynolds averaging, with the consequent need for a turbulence model to estimate the Reynolds stresses, the computational requirements are massive. Studies of two-dimensional transonic flows by, for example, Martinelli [24] have shown that for adequate resolution of a turbulent boundary layer about 32 mesh intervals are needed within the thickness of the boundary layer. A similar number of mesh intervals are needed outside the boundary layer, and in order to prevent the mesh aspect ratio from becoming excessively large in the boundary layer and wake, about 512 intervals are needed in the chordwise direction wrapping around the airfoil. Translated to three-dimensional simulations, which would also require several hundred mesh intervals in the spanwise direction over a wing, this implies the need for meshes with around 10 million points. A further extension to large eddy simulation, in which the larger eddies are calculated, while eddies smaller than the grid scale are modeled by a subgrid scale model, would require even finer meshes.

It appears that the only way in which the cost of calculations of this magnitude can be

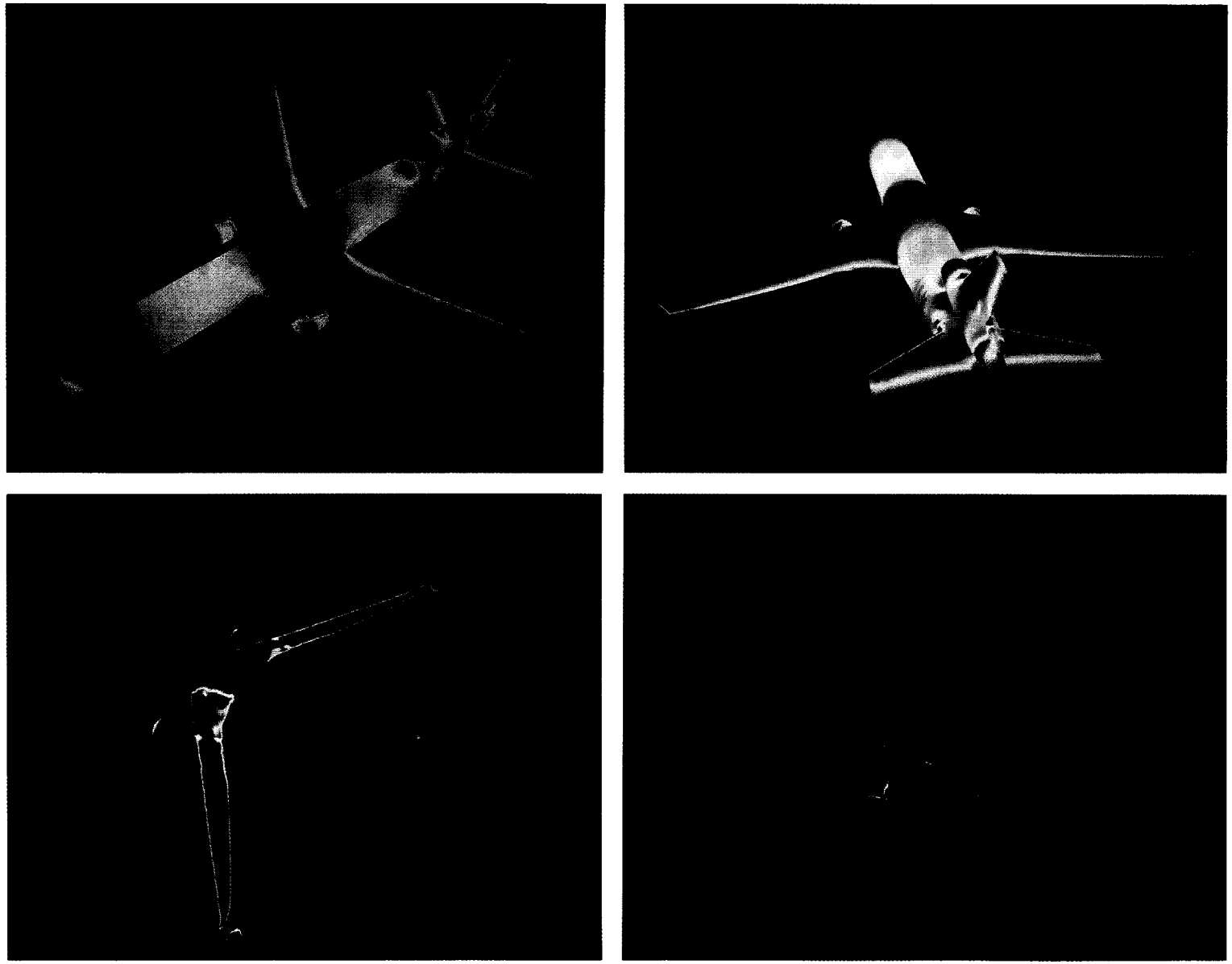

Fig. 14. McDonnell Douglas MD-11. Mach 0.825, angle of attack 2.50°. Pressure contours (top) and Mach contours (bottom).

reduced to a level acceptable for industrial use will be through the introduction of massively parallel computer architectures. This in turn requires a re-examination of the algorithms that will be needed. In this respect, the explicit methods that have been used in the present work have the advantage that they are amenable to concurrent computation at every mesh point. Very careful partitioning is needed, however, to limit the communication costs of exchanging data between different locations in the mesh. Parallel computing also offers the prospect of reducing the costs of aerodynamic analysis to the point where optimization methods of the type presented in the second part of this paper will be feasible both for more complex flow models and for three-dimensional applications. The vision of a digital wind tunnel [4] may, then, finally be brought to reality.

5. Acknowledgment

This work has benefited from the generous support of DARPA under Grant No. N00014-92-J-1796, AFOSR under Grant No. AFOSR-91-0391, and IBM.

6. References

[1] P. Arminjon and A. Dervieux, Construction of TVD-like artificial viscosities on 2-dimensional arbitrary FEM grids, INRIA Report 1111 (1989).
[2] J.P. Boris and D.L. Book, Flux corrected transport, 1 SHASTA, a fluid transport algorithm that works, *J. Comput. Phys.* 11 (1973) 38–69.
[3] M.O. Bristeau, O. Pironneau, R. Glowinski, J. Périaux, P. Perrier and G. Poirier, On the numerical solution of nonlinear problems in fluid dynamics by least squares and finite element methods (II): application to transonic flow simulations, in: J. St. Doltsinis, ed., *Proceedings of the 3rd International Conference on Finite Element Methods in Nonlinear Mechanics, FENOMECH 84, Stuttgart, 1984* (North Holland, Amsterdam, 1985) 363–394.
[4] D.R. Chapman, H. Mark and M.W. Pirtle, Computers vs. wind tunnels in aerodynamic flow simulations, *Astronautics and Aeronautics* 13 (4) (1975) 22–30, 35.
[5] G. Dahlquist, A special stability problem for linear multistep methods, *BIT* 3 (1963) 27–43.
[6] J.D. Denton, An improved time marching method for turbomachinery flow calculations, *J. Engrg. Gas Turbines Power* 105 (1983).
[7] C.W. Gear, The numerical integration of stiff ordinary differential equations, Report 221, University of Illinois, Department of Computer Science (1967).
[8] A. Harten, High resolution schemes for hyperbolic conservation laws, *J. Comput. Phys.* 49 (1983) 357–393.
[9] A. Jameson, Iterative solution of transonic flows over airfoils and wings, including flows at Mach 1, *Comm. Pure Appl. Math.* 27 (1974) 283–309.
[10] A. Jameson, Acceleration of transonic potential flow calculations on arbitrary meshes by the multiple grid method, AIAA Paper 79-1458, Fourth AIAA Computational Fluid Dynamics Conference, Williamsburg, VA (1979).
[11] A. Jameson, Solution of the Euler equations by a multigrid method, *Appl. Math. Comput.* 13 (1983) 327–356.
[12] A. Jameson, A non-oscillatory shock capturing scheme using flux limited dissipation, MAE Report 1653, Princeton University, Princeton, NJ (1984); also in: B.E. Engquist, S. Osher and R.C.J. Sommerville, eds., Lectures in Applied Mathematics 22 (American Mathematical Society, Providence, RI, 1985) 345–370.
[13] A. Jameson, Multigrid algorithms for compressible flow calculations, in: W. Hackbusch and U. Trottenberg, eds., *Proceedings of the 2nd European Conference on Multigrid Methods, Cologne, 1985*, Lecture Notes in Mathematics 1228 (Springer, Berlin, 1986) 166–201.

[14] A. Jameson, Successes and challenges in computational aerodynamics. AIAA Paper 87-1184-CP, AIAA 8th Computational Fluid Dynamics Conference, Honolulu, HI (1987).
[15] A. Jameson, Aerodynamic design via control theory, *J. Sci. Comput.* 3 (1988) 233–260.
[16] A. Jameson, Automatic design of transonic airfoils to reduce the shock induced pressure drag, in: *Proceedings 31st Israel Annual Conference on Aviation and Aeronautics*, Tel Aviv (1990) 5–17.
[17] A. Jameson, Time dependent calculations using multigrid, with applications to unsteady flows past airfoils and wings, AIAA Paper 91-1596, AIAA 10th Computational Fluid Dynamics Conference, Honolulu, HI (1991).
[18] A. Jameson, T.J. Baker and N.P. Weatherill, Calculation of inviscid transonic flow over a complete aircraft, AIAA Paper 86-0103, AIAA 24th Aerospace Sciences Meeting, Reno, NV (1986).
[19] A. Jameson, W. Schmidt and E. Turkel, Numerical solutions of the Euler equations by finite volume methods with Runge–Kutta time stepping schemes, AIAA Paper 81-1259 (1981).
[20] B. Laney and D.A. Caughey, Extremum control II: semi-discrete approximations to conservation laws, AIAA paper 91-0632, AIAA 29th Aerospace Sciences Meeting, Reno, NV (1991).
[21] M.J. Lighthill, A new method of two dimensional aerodynamic design, R & M 1111, Aeronautical Research Council (1945).
[22] J.L. Lions, *Optimal Control of Systems Governed by Partial Differential Equations* (Springer, New York, 1971); translated by S.K. Mitter.
[23] M.-S. Liou and C.J. Steffen, A new flux splitting scheme, NASA-TM 104452 (1991); also: *J. Comput. Phys.* (to appear).
[24] L. Martinelli and A. Jameson, Validation of a multigrid method for the Reynolds averaged equations, AIAA Paper 88-0414 (1988).
[25] O. Pironneau, *Optimal Shape Design for Elliptic Systems* (Springer, New York, 1984).
[26] P.L. Roe, Approximate Riemann solvers, parameter vectors, and difference schemes, *J. Comput. Phys.* 43 (1981) 357–372.
[27] J.L. Steger and R.F. Warming, Flux vector splitting of the inviscid gas dynamic equations with applications to finite difference methods, *J. Comput. Phys.* 40 (1981) 263–293.
[28] R.C. Swanson and E. Turkel, On central-difference and upwind schemes, *J. Comput. Phys.* 101 (1992) 297–306.